Mekelle University

Ethiopian Institute of Technology, EiT_M

School of Electrical and Computer Engineering

MSc. Program in Communication Engineering

Final Thesis Acceptance Form

1. Name: **Tedros Tilahun** ID: **EITM/PE064/10**
2. Thesis Title **Angle of Arrival Estimation using Hybrid Rat Race Coupler for Close-Spaced Patch Antenna Array Utilizing SRR Metamaterial Superstrate**
3. This is to certify that Mr. **Tedros Tilahun** has incorporated all the comments forwarded to him by the external and internal examiners during the thesis defense held on 05 11 2024.

3.1 Tedros Tilahun (Student)	Signature	Date
3.2 Tekle Birhane (Asst. Prof) (Advisor)	Signature	11/12/2024 Date
3.5 G/medhin Wubet. (Asst. Prof) (Internal Examiner)	Signature	11/12/2024 Date
3.4 Dr. **Gebrekiros Gebreyesus** (External Examiner)	Signature	12-11-2024 Date
3.5 Adhana Nigus (School Head, ECE)	Signature	14-11-2024 Date

School of Electrical & Computer Engineering
Ethiopian Institute of Technology-Mekelle

MEKELLE UNIVERSITY

ETHIOPIAN INSTITUTE OF TECHNOLOGY-MEKELLE

School of Electrical and Computer Engineering

Angle of Arrival Estimation using Hybrid Rat Race Coupler for Closely-Spaced Patch Antenna Array Utilizing SRR Metamaterial Superstrate

A Thesis Submitted in Partial Fulfillment of the Requirement for the **Degree of Masters of Science in Communication Engineering**

By

Tedros Tilahun

Advisor

Tekle Brhane (Ass. prof.)

Declaration

I, the undersigned, declare that this thesis work is my original work, has not been presented to any other university or institute for the award of any degree or diploma so far, and all sources of material used for the thesis work have been fully acknowledged.

Name of student Signature

Place: Mekelle

Date of Submission

This thesis has been submitted for examination with my approval as a university advisor.

Tekle Birhane (MSc.)

Advisor's name Signature

Acknowledgements

I would like to convey my utmost gratitude to my advisor, Tekle Birhane, for his hands-on expertise, generous guidance and support throughout the completion of this work. He has always welcomed any questions I had at any place, and we would discuss enthusiastically by exploring different questions in the realm. It has been a profound experience to work with a great mentor

Last but not least to my family and friends who were on my side throughout the journey, my gratitude is the deepest.

Abstract

Estimating the angle of arrival (AoA) of a coming signal can accomplished using various methods. In most cases algorithms are used for such purposes. However, algorithms are naturally complicated and expensive, and also cause a degradation in system performance. Therefore, other methods such as, 180^0-hybrid rat race (HRR) coupler can be applied for effectively estimating the AOA of a coming signal.

In this thesis work, an 180^0 HRR coupler integrated with a 2x1 closely-spaced patch antenna array and a negative permeability metamaterial was studied for estimating AoA of a coming signal. The 180^0 HRR was made up of a ring metallic sheet integrated with four additional branches placed at the edges of it. It operates at 10 GHz so as to make compatible with the 2x1 patch antenna array's operating frequency. The simulation results show, the 180^0 HRR coupler is characterized by 0^0-phase at the sum (Σ)-port while 180^0 phase shift at the difference (Δ) port at the given operating frequency. In order to integrate with the 180^0 HRR, a 2x1 array patch antenna with an inter - element distance of 0.6λ (where λ is the operating wave length) was designed. The antenna array workes at 10GHz with a maximum simulated gain of 8.824 dB *while keeping the mutual coupling to a minimum of -23 dB. To further achieving miniaturization, the inter-element distance reduced to 0.4λ. The simulation result shows a resonance at 10 GHz frequency and maximum gain of 7.8 dB while the mutual coupling increased to -9 dB. The 2x1 patch antenna array with inter - element distance of 0.6λ -180^0 HRR coupler system was able to estimate the AoA of the received signal from 0^0 to 19^0 with error of less than 5^0. While with a reduced inter – element distance to 0.4λ, the system was able to estimate signals from 0^0 to 50^0 with error of less than 5^0. Upon integrating split ring resonator (SRR) metamaterials, mutual coupling reduced to -15.6 dB without affecting the AOA of the system. This study was able to estimate AOA in a wide range of an incoming signal while keeping the inter – element distance smaller.*

The proposed design can be applied in radar system applications where accurate estimation of AOA of an incoming signal is needed such as in target tracking, surveillance, and navigation missions.

Table of Contents

List of Abbreviations

AoA----------Angle of arrival

SRR----------Split Ring Resonator

HRR----------Hybrid Rat Race Coupler

CGM----------conjugate gradient method

LMS---------- least mean square

SMI---------- sample matrix inversion

RLS---------- recursive least square

ESPRIT----------signal parameters with rotational invariance technique

NRM----------Newton–Raphson method

DSM---------- delay and sum method

MUSIC---------- multiple signal classification

CST----------computer simulation software

EM---------- electromagnetic

SRR---------- split ring resonator

List of Tables

List of Figures

Chapter One

Introduction

1.1 Background

The radiation pattern of a coming signal has maximum power at the center of the lobe and gets gradually decrease at the edges [1]. The receiver antenna should be designed so that it captures maximum power of the transmitted signal. This is accomplished in estimating the angle of arrival (AoA) of a coming signal properly. Estimation of AoA is important for various applications such as Radar and Satellite communications [2]. To estimate the AoA of a coming signal various technique has been applied. In most cases, algorithms have been applied for the estimation purposes.

The AoA estimation also can be accomplished using180^0 HRR coupler in integrating with different array antennas. The array antennas used to capture the coming signal and added or subtracted the phase at the coupler. However, mostly the array antennas are configured only considering the effect of mutual coupling which could occur among elements of the array. Such consideration affects the compactness of the design and might not feasible in integrating with electronics circuits.

Metamaterials has important applications across wide range of applications. Notably, metamaterials can be applied to achieve compactness while keeping the performance of array antennas. Metamaterials are artificially engineered structures which possess unique properties when EM wave propagate through it. Metamaterials also called left-handed materials [3].

In this proposed design, an 180^0 HRR coupler integrated with 2x1 patch antenna array and negative permeability metamaterial split ring resonator (SRR) was employed to estimate the AoA of a coming signal. The 180^0 HRR coupler operates at 10 GHz so as to make compatible with the 2x1 patch antenna array's operating frequency. At the same time, the SRR metamaterial exhibits negative permeability at the mention operating frequency. This proposed work can be deployed in radar application for estimating angle of arrival of received signal with accuracy and precision.

1.2 Literature Review

In designing receiver antenna, the quality of the signal on the main lobe and the direction it is receiving the signal is important to take into account. This is where the AOA estimation has important factor.

In [4], analysis of adaptive beamforming algorithms for smart antennas is studied. The performance is studied by varying the inter element spacing and number of antenna elements. The inter -element separation distance has been determined as 0.5λ. But, the complexity of the system limits the proposed design.

Moreover, A. S. e. al. [5], presented a comparative study of beam forming techniques using different algorithms is reported. The accuracy of the techniques is measured based on the angle of arrival. The LMS algorithm shows better performance across range of angles of arrival. Despite reporting better performance, the overall size of the system makes the deployment cost expensive.

Likewise, in [6] a study of adaptive algorithms in relation to performance in smart antenna designs reported. A good result for the mean square error is reported by using the Kalman based normalized Least Mean Square algorithm. Despite the reduced mean square error reported, the proposed work suffers from high complexity of the system.

On the other hand, smart antennas along with other algorithms such as, estimation of signal parameters with rotational invariance technique (ESPRIT) [7] is applied to estimate the AoA of a coming signal. Though, wide range of the AoA abled to measure, the system is not applicable for miniaturization purposes.

The sum and difference co-array method were applied to estimate the degree of freedom of an array configuration in the work presented in [8]. This attempt was enabled to enhance the degree of freedom of the proposed work though a costly from deployment point of view.

On a related work [9], genetic algorithm was applied to estimate the direction of arrival of a coming signal. The reported algorithm showed better accuracy particularly in low SNR and closely spaced array of antennas. However, the system introduces complexity which results in increased cost. In [10], a Capon estimator was used to estimate the power by combining noise and signal from

different directions. Despite its large size, it reported better spatial resolution compared to other existing algorithms.

By collecting signal characteristics for robot applications [11]; where the robot estimates position based on the direction of arrival of the signal was measured. Up to 30 degrees of DoA with a less estimation error was reported. Nonetheless, the system demands huge resource in terms of space and energy.

A virtual multi antenna array [12] are proposed for DoA estimation purpose using the local osillator frequency. It reported a wide range of angle of arrival estimation with small mean square error. In a similar work ausing Deca-wave DW1000 integrated circuits is proposed to measure the angle of arrival of a coming signal [13]. It reported a wide range of angle of arrival with small least mean square error. On top of that, to enhance signal capturing capability of the antenna array, a rotational directional antenna array [14] is proposed. On the other hand, a parasitic array [15] for purpose of angle of arrival estimation is reported. Despite the fact that switching and rotational arrangement of the array improve the performance, it makes the systems circuit bulkier and more expensive.

A sum-difference method for finding the angle of arrival of a signal is presented in [16]. It reported the integration of digital communication systems with direction finding method in a way of reverse mono-pulse. A space-time adaptive processing radar combined with sum and difference method for beam forming purposes is reported in [17]. The reported work presented a robust system against jamming contamination as well as performance in the Doppler and angle accuracy is reported. However, the system introduced complex number of elements that could consume much power and cost.

In other approaches, single patch antenna with mono-pulse patterns is studied in the estimation of the AoA is utilizing the sum and difference in 180° HRR coupler [18] . Wide range of angle of arrival of the system is reported by including the sum and difference method. However, the reported gain is small, and this limits the antenna's application, particularly in high gain demanding applications.

On the other hand, a 2x1 array patch antenna integrating with HRR coupler is presented [19]. Better performance in terms of the gain, least mean square error, and efficiency is observed. However, the large inter- element space between the antennas contributes for occupying large space. This makes the proposed work not suitable to use in applications that need miniaturized components. Four antennas elements [20] are applied to estimate AOA of an incoming signal. The study achieved a 1.86^0 average angle of estimation error for a direction from -60^0 to 60^0. Notwithstanding the performance is good, the number of antennas consume more power and also add complexity to the system. Likewise, AOA estimation for a frequency-hopping cooperative object is discussed in [21]. This study utilized a Fourier bandpass filter and multiple signal classification (MUSIC) methods. The study reported the root mean square error (RMSE) estimation about 1^0. However, the use of multiple algorithms introduces a delay to a given antenna system. Other latest studies such as [22], apply machine learning combined with signal processing methods to estimate the AOA. This study reports a 20% improved performance comparing other traditional tools. Despite the reported performance, the regression methods encounter various drawbacks. Similarly, in [23] transfer learning method was used to estimate the angle of arrival of an incoming signal. The study reported a better performance in terms of the angle of arrival though the method by itself increases complexity.

The overall summery of related literatures is provided in Table 1.1.

Table 1.1: Review existing literatures

Ref	Method	Achieved	Gap
[4]	varying the inter element spacing between number of antenna elements	An optimal inter - element separation distance reported 0.5λ	Complex circuitry
[5]	LMS algorithm	LMS algorithm shows better performance	Demand high cost

		across range of angles of arrival	
[6]	adaptive algorithms	Small mean square error	Complexity of the system
[7]	rotational invariance technique	abled to measure wide range of the AoA	Huge power
[8]	sum and difference co-array method	enhance the degree of freedom	Large size
[9]	genetic algorithm	better accuracy particularly in low SNR	Demand high huge resource
[10]	Capon estimator	better spatial resolution	Complexity of the system
[11]	collecting signal characteristics	30 degrees of DoA with a less estimation error	Demand high space and energy
[12]	local osillator frequency	reported a wide range of angle of arrival estimation	costly
[13]	Deca-wave DW1000 integrated circuits	small least mean square error	circuit bulkier and more expensive
[14]	rotational directional antenna array	enhance signal capturing capability	Occupies large space

[15]	parasitic antenna array	Improved AOA estimation performance	expensive
[16]	sum-difference method	integration of digital communication systems with direction	circuit bulkier and more expensive
[17]	space-time adaptive processing radar combined with sum and difference method	robust system against jamming contamination	Demand high space
[18]	single patch antenna with mono-pulse patterns	Wide range of angle of arrival	Small gain
[19]	2x1 array patch antenna integrating with HRR coupler	Better performance in terms of the gain,	large inter-element space between the antennas
[20]	Using four identical antenna elements	Better performance in MSE error	Use of large number antennas
[21]	Fourier bandpass filter and multiple signal classification (MUSIC) methods	performance in RMSE error	Use of multiple algorithms
[22]	machine learning combined with signal processing methods	reports a 20% improved performance	regression methods encounter various drawbacks
[23]	transfer learning method	reported a better performance	increases complexity

From the existing literatures, it is evident that various methods are employed to estimate the AoA. However, each method has its own limitations. The switched and scanning antennas have complexity in implementation of the system. Also, the adaptive beam forming and smart antenna estimation have computational complexity of the algorithms applied. In the spatial distribution of AoA estimation, the accuracy is below the margin. To address the limitations of various approaches, a more efficient and better approach is presented in this proposed design. A 2×1 patch antenna array working at 10 GHz is integrated with an HRR coupler-SRR metamaterial combination, to utilize the sum and difference method of the received signal for the estimation.

1.3 Statement of the Problem

The estimation of AoA with the help of HRR and array antenna elements is important in its aspect. However, the distance between the array antenna elements is still a stressing factor. If the distance is taken as the conventional distance, then the space becomes large as a result, designing compact antenna makes it difficult. On the other hand, if the distance considered is less than the conventional, mutual coupling effect degrades the performance of the array antenna.

Considering the existing limitation, to get a more compact, gain enhanced, more directive as the same time estimating the angle of arrival from the array antenna can be designed by combining the hybrid rat race coupler (HRR) and negative permeability metamaterials.

1.3 Objectives

1.3.1 General objectives

The main objective of the thesis is to estimate the angle of arrival (AOA) of incoming signal using 180^0 hybrid rat race (HRR) coupler coupled with a closely-spaced 2x1 patch antenna array based on negative mu- metamaterial.

1.3.2 Specific objectives

The following specific objectives are addressed in the Thesis work:

- ✓ Design of an 180^0 HRR coupler integrated with 2x1 patch antenna array, and estimate the AOA for inter - element separation distance, ($d = 0.6\lambda, 0.4\lambda$)
- ✓ Design of an 180^0 HRR - 2x1 patch antenna with negative mu- metamaterial unit cell array, apply simulation, analysis, and estimate the AOA for inter - element separation distance, ($d = 0.4\lambda$)
- ✓ Obtain the performance of AoA of the proposed design, make discussions, and reached at conclusions from the simulation results

1.4 Methodology

To accomplish the proposed design, several methods were used. The first method was collecting literatures related to the topic. Reading the literatures and clearly identifying the limitations and achievements in the existing literatures. Clearly understanding the concepts behind the 180^0 coupler, patch antenna, and metamaterials, the idea of AoA was another aspect of the work. The final task was identifying the platform for simulations and modelling. CST software was selected for modeling and simulation of the all designs while MATLAB was selected for plotting the normalized power and AoA of the received signal by the 180^0 HRR coupler. For the sake of brevity, all the methods are put in flow chart of Figure 1.1.

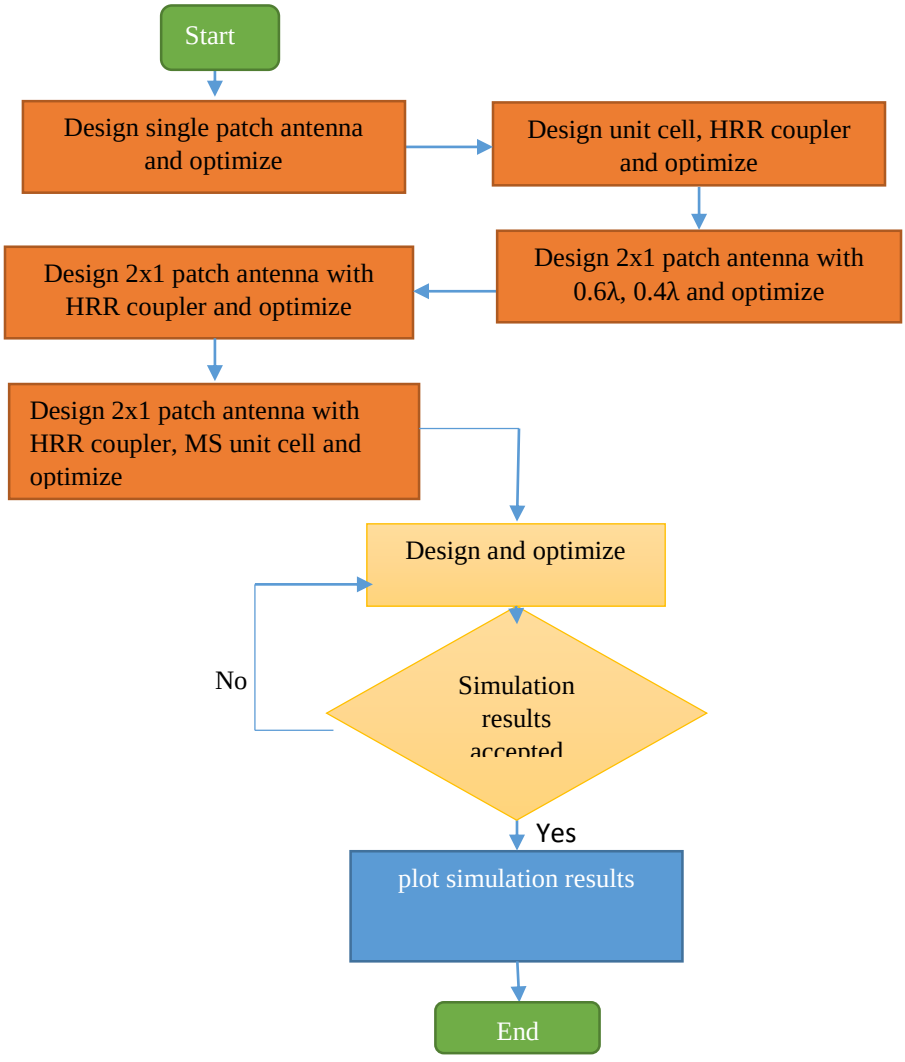

Figure 1.1: Methodology flow chart

1.5 Thesis Layout

This thesis work is organized as follows. In Chapter 1, the background, literature review, statement of the problem, methodology and objective of the work are discussed. Chapter 2 discusses about the theoretical concepts of antennas, angle of estimation, and 180^0 HRR coupler working principles. The system model and its details are described in Chapter 3. Chapter 4 deals about the obtained simulation results and the discussion. Chapter 5 is the conclusion and discussion part of the work.

Chapter Two

Application of HRR Coupler in Conjunction with Antennas in Angle of Arrival Estimation

2.1 Antenna Theory

An antenna is a metallic conductor which receives or transmits electromagnetic (EM) waves in communication systems. Antennas operate from low frequency (LF) to very high frequency (VHF) electromagnetic (EM) spectrum. They either convert EM waves to current and voltage (in receiving mode) or current and voltage to EM waves (in transmitting mode). On the other hand, antennas are transitional elements between the free space and guiding structure [24]. In a wireless communication system, the performance of antenna affects the overall system.

In a transmitting mode, an antenna system is modelled in transmission-line Thevenin equivalent as indicated in Figure 2.1. The source is represented by ideal generator, Vg, the transmission line is modelled as a line with characteristics impedance z_c, and the antenna is represented by a load Z_A (2.1) [24],

$$Z_A = (R_L + R_r) + jX_A \quad \text{.......} \quad (2.1)$$

R_L, represents the conduction and dielectric losses associated with the antenna structure, while R_r and X_A represent radiation resistance and imaginary part of reactance by the antenna respectively.

There will be maximum transfer of power from the source (generator) to the load (antenna) as long as there is conjugate matching condition between the characteristic's impedance of the transmission line and the load impedance (i.e antenna impedance).

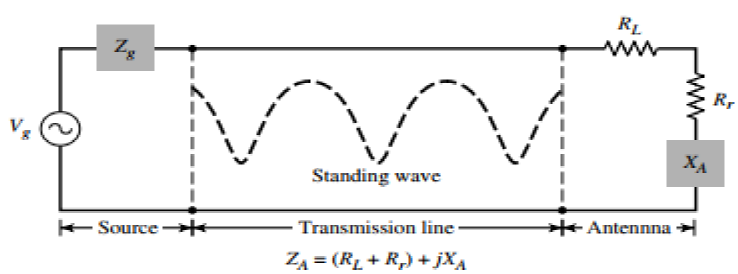

Figure 2.1: Transmission Thevenin equivalent of antenna in transmitting mode [24]

Notwithstanding, the working principle of antennas is the same, they could have different forms to meet certain demand. They are designed in single wire (monopole), two-wire (di-pole), planar (patch), or reflector forms.

2.1.1 Planar (Patch) Antennas

Patch antennas are the most used type of antennas since they are easy to design in low profile, compatible in planar and nonplanar surfaces, simple and inexpensive to fabricate using printed-circuit technology [24].

There are three main components in patch antenna system, as shown in Figure 2.2, a patch is placed on top of the substrate, the substrate is placed above ground plane [24]. The antenna is placed so that its maximum radiation pattern is normal (broadside) to the patch. The working principle of patch antenna is simple; electromagnetic waves are first guided along the coaxial or microstrip strip-line and then spread out under the patch. When they reach the boundary of the patch, some are reflected and some radiate into open space.

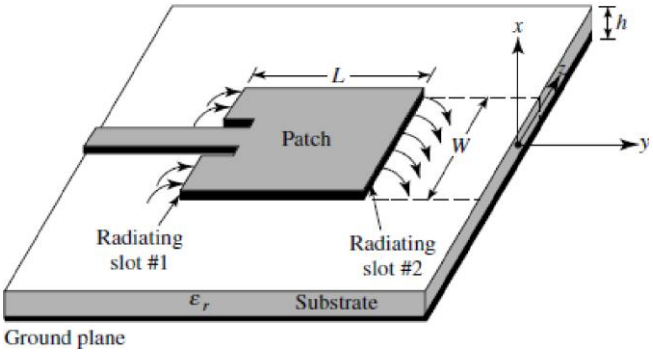

Figure 2.2: Patch antenna [24]

2.1.2 Patch Antenna Model

There are different types of patch antenna models. In this work, for brevity, only the transmission line model is discussed.

2.1.2.1 Transmission-Line Model

Transmission line model is the most common method in the design of patch antennas. However, it suffers from less accuracy. In this method of analysis, the patch antenna is represented by two slots separated by a transmission line with length L and characteristics impedance, z_C [24].

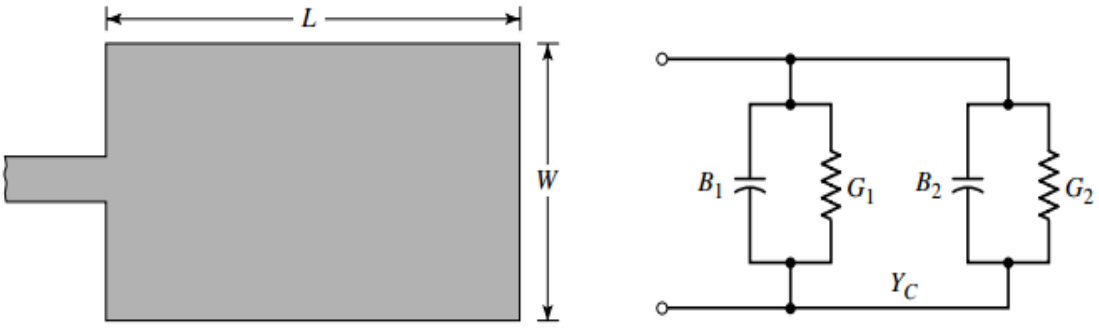

(a) Rectangular patch (b) Transmission model equivalent

Figure 2.3: Rectangular microstrip patch and its equivalent circuit transmission-line model [24]

In the use of transmission line method of analysis, the following equations are applied [24].

First, the effective dielectric constant, ϵ_{reff} is derived as

For $\frac{w}{h} > 1$

$$\epsilon_{reff} = \frac{\epsilon_r+1}{2} + \frac{\epsilon_r-1}{2}\left[1 + 12\frac{h}{w}\right]^{-\frac{1}{2}} \quad \text{.....(2.5)}$$

$$L = \frac{1}{2f_r\sqrt{\epsilon_{reff}}\sqrt{\mu_0\epsilon_0}} - 2\Delta L \quad \text{..... (2.6)}$$

Here, ΔL is obtained as [25]

$$\Delta L = 0.412\frac{(\epsilon_{eff}+0.3)\left(\frac{w}{h}+0.264\right)}{(\epsilon_{eff}-0.258)\left(\frac{w}{h}+0.8\right)}h \quad \text{..... (2.7)}$$

Because of the fringing effect, length of the patch is extended by ΔL on each side. Hence, effective length of the patch is determined as

$$L_{eff} = L + 2\Delta L \quad \text{..... (2.8)}$$

To obtain a good radiation efficiency is, the width is calculated as [20]:

$$W = \frac{1}{2f_r\sqrt{\mu_0\epsilon_0}}\sqrt{\frac{2}{\epsilon_r+1}} \quad \text{..... (2.9)}$$

Where, μ_0, and ϵ_0 permeability and permittivity of the free space respectively.

During patch antenna designs, it is important knowing that length of the patch controls the resonant frequency and the width of the patch affects the impedance level at resonance.

2.1.4 Feeding Techniques (Methods)

In the analysis of patch antennas, different methods of feeding are used. The most used techniques are; microstrip, coaxial, aperture coupling, and proximity coupling feed techniques [25]. Applying such methods have their own advantages and disadvantages.

2.1.4.1 Microstrip Line Feed

Microstrip line feed is easy to design, simplest achieving the matching condition of all the feed methods. The microstrip feed line is always conducting strip, with the width being much smaller compared to the patch. This method is applied in two different ways of integrating the microstrip line to the patch. Microstrip line edge with inset and quarter wave transformer (QWT) feed technique.

The inset feed method the strip line is integrated with the patch by cutting out small parts from the antenna carefully as shown in Figure 2.4 [24]. Whereas, the quarter wave transformer (QWT) uses two microstrip lines to match the characteristics impedance of the line to the load (patch) as shown in Figure 2.5. The formula to determine the width and length dimensions of the microstrip line are available in antenna books and different literatures. In this thesis QWT is used to feed the patch and the AoA of the antenna part.

However, microstrip line feed method is has limited bandwidth due to surface waves and increment of spurious feed radiation as the height of the substrate increases [24].

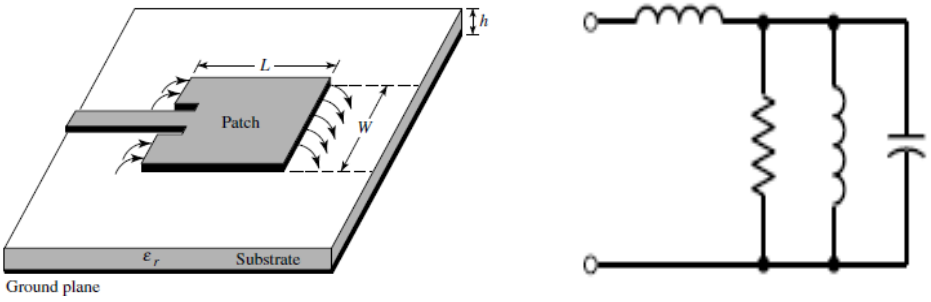

(a) (b)

Figure 2.4: Patch antenna feed technique (a) Microstrip line feed model (b) Equivalent circuit [24]

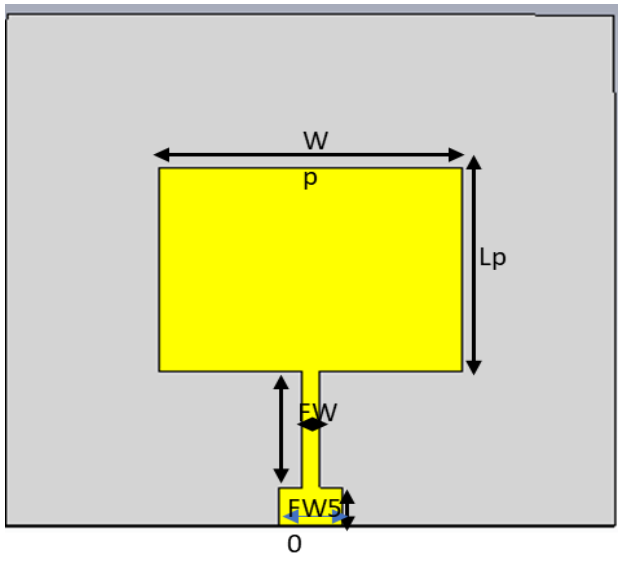

Figure 2.5: Patch antenna with quarter wave transformer feed technique [taken from Chapter 3]

2.1.4.2 Coaxial Probe

In coaxial feeding technique, the outer conductor of the feed is connected to the ground plane of the microstrip antenna. Part of radius the same as the internal conductor is removed from the ground. The internal conductor passes through the dielectric substrate and connects to the patch [26]. The inductance effect of the probe shifts the resonant frequency upward slightly.

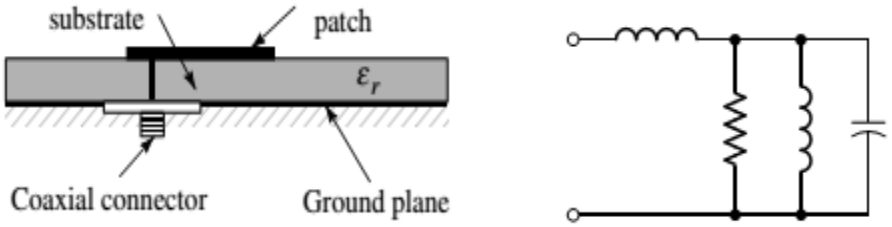

Figure 2.6*:* Patch antenna feed technique (a) Coaxial feed model (b) Equivalent circuit [27]

2.1.4.3 Aperture Coupling

Two substrates separated by a common ground are applied in aperture coupling feed method. The microstrip line on the lower substrate is electromagnetically coupled to the patch through a slot aperture in the common ground as shown in Figure 2.7a [27]. The aperture coupling is difficult to fabricate and has narrow bandwidth. However, in case of modelling, it is easier to model and has

moderate spurious radiation [27]. The non-resonant slot is represented by an inductor in series with R-L-C circuit of the patch as shown in Figure 2.7b.

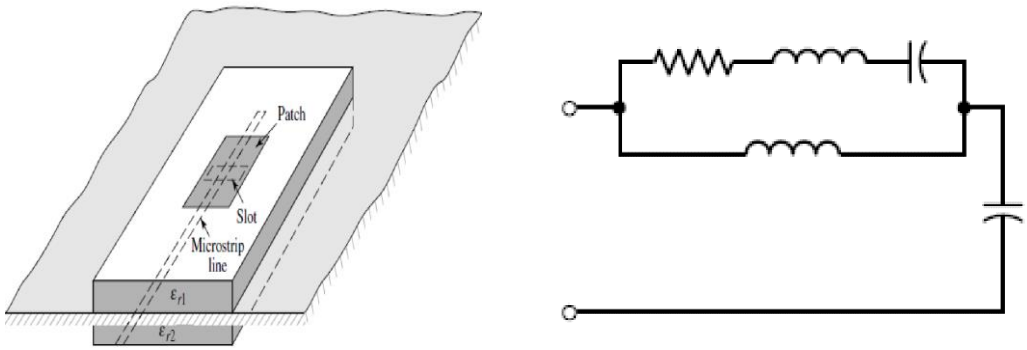

(a) (b)

Figure 2.7: Patch antenna feed (a) Aperture coupling feed model (b) Equivalent circuit [27]

2.1.4 Antenna Basic Parameters

2.1.4.1 Return Loss

Return loss measures the degree of mismatch between the transmission line's characteristic impedance and antenna impedance. Whenever a mismatch occurred between the transmission line and antenna, part of the power reflected back from the load (antenna) to the transmission line. The return loss of an antenna is measured in dB. Mathematically, it is described as [28]**:**

$$R_L=-20|\Gamma| \quad \text{....} \qquad (2.10)$$

where the $|\Gamma|$ is the magnitude of the reflection coefficient. It is the ratio of the partly reflected wave to the incident wave and its magnitude is in between 0 and 1. For a good impedance match the return loss is always specified as -10dB and less for antenna engineering designs.

2.1.4.2 Input Impedance

For proper design of antennas, the input impedance of the antenna should match with the characteristics impedance of the transmission line so that power from the source is delivered to the load (antenna) and reflection of power is minimized. The characteristic impedances of

transmission lines are commonly 50Ω or 75Ω. Hence, the designed antenna input impedance should be specified as 50Ω or 75Ω [26].

2.1.4.3 Bandwidth

This parameter describes the range of frequencies of over which the antenna can work properly. Antennas operate in narrower bandwidth or wider band-width based on the nature and desire of the application.

2.1.4.4 Gain

Gain combines the radiation efficiency and directivity of an antenna system. It measures how an antenna converts a given input power to radio waves that propagate to space in a desired direction. Mathematically it is defined as [20];

$$G = \frac{4\pi U}{P_{in}} \quad \text{..... (2.11)}$$

Where U is radiation intensity and P_{in} is the input power to the antenna.

2.2 Angle of Arrival (AoA) Estimation

In some wireless communication areas, estimating the direction of received signal is necessary. More specifically, in radar communication system, the received signal's angle of arrival is crucial in detecting the target. In this work, a 180 HRR coupler is proposed to estimate the angle of arrival from 2x1 array patch antennas. A coupler when fed two of its branches, it produces sum and difference of the received signal as the following equations [29]:

$$\Sigma = 1 + e^{-jkd\sin\theta} \text{.....(2.12)}$$

$$\Delta = 1 - e^{-jkd\sin\theta} \text{.....(2.13)}$$

Applying mathematical iteration, AoA is obtained as the equation [29]:

$$\theta = \sin^{-1}\left(\frac{\lambda}{\pi d}\tan^{-1}\frac{\Delta}{\Sigma}\right) \text{..... (2.14)}$$

Where d, is inter element distance between antenna array, and λ is the free space wave length.

2.2.1 Working principle of 180^0 Hybrid Rat Race Coupler

The 180^0 HRR coupler, is a type of coupler commonly used in RF/microwave devices. As shown in Figure 2.8, the coupler consists of four branches with the distance between the bottom part of the branch of $\frac{3\lambda}{4}$ and the rest consecutive branches $\frac{\lambda}{4}$ (where λ is the operating frequency wave length) apart. The ring part has a characteristic impedance of $\sqrt{2}$ times the branch impedance, for instance, for 50 Ω branch impedance, the ring impedance is $\sqrt{2}$*50=70.7 Ω. The overall circumference of the coupler ring is equal to 1.5λ. Moreover, the ring of coupler consists of six sections with each section length equals to L, (where L= $\lambda/4$). Therefore, the radius r, of ring can be obtained using the following expression [30].

$$r = \frac{360\ L}{2\pi C} \quad \text{(2.15)}$$

Where C, is the angle in degree [31], in this case, C is 60 degrees for each section. Hence the equations for the ring, and four branches are calculated as follow [30]:

$$\beta = \frac{377\pi}{2Z_0\sqrt{\varepsilon_r}} \quad \text{(2.16)}$$

Where, β is the phase constant, Z_0 is the characteristics impedance of the branch and ring lines while ε_r is the relative permittivity of the dielectric.

The width of each branch of the coupler is obtained as in [30]:

$$\frac{W}{h} = \frac{2}{\pi}\left[\beta - 1 - \ln(2\beta - 1) + \frac{\varepsilon_r - 1}{2\varepsilon_r}\left\{\ln(\beta - 1) + 0.39 - \frac{0.61}{\varepsilon_r}\right\}\right] \quad \text{(2.17)}$$

The working principle is; input signals in ports-3 and -4, travels in opposite direction and reach the sum port (port-1), traveling a distance of λ/4 that contributes to a phase shift of 90° in each of the input signals [30]. However, because of traveling in opposite directions, the phase difference between the two input signals gets canceled, and the net phase change between the two input signals at the sum port (Σ) is zero. The input signal from port-4 travels a distance of $\frac{3\lambda}{4}$ to reach the difference port-2 (Δ-port), while the input signal from port-3 travels a distance of $\frac{\lambda}{4}$ to reach the difference Δ-port. A distance of $\frac{\lambda}{2}$ which corresponds to a phase difference of 180° between the two input signals at the difference port-2 (Δ-port). This is going to be discussed in Chapter 4 by supporting with simulation results of HRR coupler.

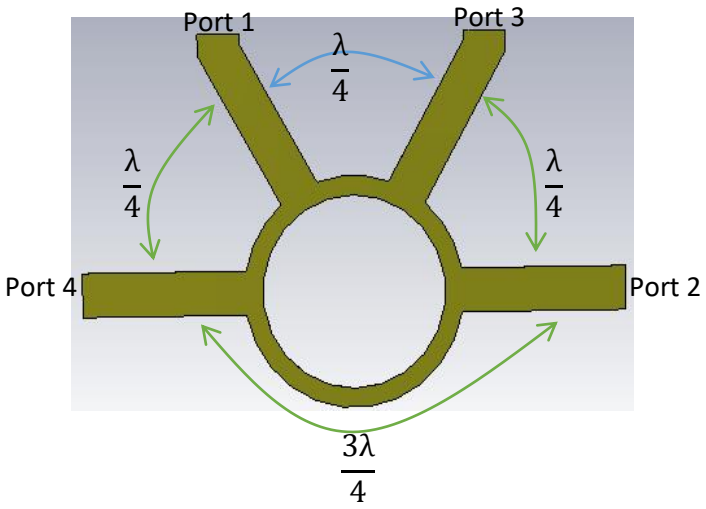

Figure 2.8: 180^0 HRR coupler

2.3 Angle of Arrival Estimation using Hybrid Rat Race Coupler Utilizing SRR Metamaterial Superstrate and Application Areas

The hybrid rat race coupler (HRR) is an ideal microwave component for splitting or combing microwave signals. When it is combined with 2x1 patch antennas, it enables to add or subtract the phase of a coming signal. As a result, it is ideal for estimating the angle of arrival of a receiving signal. It gives even further benefit when it is integrated with the square split ring resonator (SSRR). The main challenge in the design of antenna arrays is the mutual coupling induced in adjacent antenna elements when the inter element distance is less than 0.5λ. Due to this problem, it is difficult to design more compact antennas. However, by applying SSRR metamaterial unit cells, it is possible to resolves such problem. When the SSRR array elements are placed at some height of the antenna elements, it is possible to suppress the interfering coupling from one element to other antenna element. This method enabled to design a novel work where the inter – element distance is 0.4λ. The proposed design provides two benefits; while it is compact is size it also enables to estimate angle of arrival for incoming signals. Having stated its characteristics, the proposed work can be applied for various purposes such as:

- ✓ Satellite Communication
- ✓ Military and Defense Systems
- ✓ Wireless Communication Systems

- ✓ Radar and sensing Systems
- ✓ Navigation and Localization
- ✓ Remote sensing and monitoring

Chapter 3

System Model

In this chapter all the models of the design are discussed in detail. Before developing the models in CST software, all the required parameters were selected. The basic parameters that determine

the dimensions of the model i.e. operating frequency, height of the substrate, and permittivity of the substrate were specified as it will be discussed on the next section. Based on this notion, models for single rectangular patch antenna, 2x1 rectangular patch antenna array, square SRR, and 180^0 HRR coupler were developed. Moreover, the model for the final step of the work i.e. 2x1 rectangular patch antenna integrated with the 180^0 HRR coupler in conjunction with square SRR superstrate was designed.

3.1. 180^0 Hybrid Rat Race Coupler Model

The layout of the model is developed based on the previous formulas discussed in Section 2.2.1. Applying the mathematical equations, the initial dimensions of the HRR coupler were obtained thereby the layout of the model drawn in CST software. However, to obtain the desired result at 10 GHz operating frequency, Trust Region Framework (TRF) optimization method which is available in CST was applied. After completing the optimization process, dimensions of the HRR coupler were obtained as listed in Table 3.1.

Table 3.1*:* HRR coupler design parameters and optimized values

Parameter	dimension
Operating frequency (f)	10 GHz
Permittivity of the substrate (ε_r)	3.23
Substrate height (hs)	0.85 mm
Inner radius (r_{in})	4.11 mm
Outer radius (r_{out})	4.94 mm
Width of ports (w)	1.87 mm
Substrate width (Ws)	4.23* r_{out}
Substrate length (Ls)	2* r_{out}

Based on the parameters the layout of the design is shown in Figure 3.1. In the 180 ° HRR coupler layout, the larger section has a length of $\frac{3\lambda}{4}$ and the rest with $\frac{\lambda}{4}$ electrical length. However, all the branches are equal in length in order to exist coherent propagation of the EM wave in the coupler. The dimension of the model was selected so that it satisfies the working principle of the 180^0 HRR coupler. The working principle is; input signals in ports-3 and -4 as shown in Figure 3.1, travels

in opposite direction and reach the sum port (port-1), traveling a distance of λ/4 that contributes to a phase shift of 90° in each of the input signals. However, because of traveling in opposite directions, the phase difference between the two input signals gets canceled, and the net phase change between the two input signals at the sum port (Σ) is zero. The input signal from port-4 travels a distance of $\frac{3\lambda}{4}$ to reach the difference port-2 (Δ-port), while the input signal from port-3 travels a distance of $\frac{\lambda}{4}$ to reach the difference Δ-port. A distance of $\frac{\lambda}{2}$ which corresponds to a phase difference of 180° between the two input signals at the difference port-2 (Δ-port). This is going to be discussed in Chapter 4 by supporting with simulation results of HRR coupler.

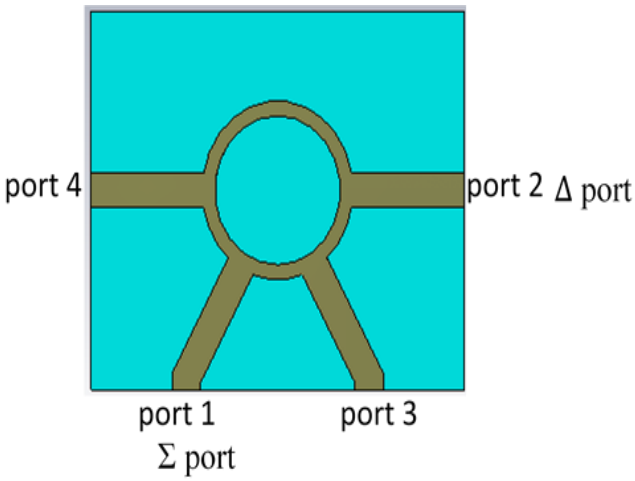

Figure 3.1: HRR coupler layout

3.2 Rectangular Patch Antenna Model

To measure the performance of the coupler and obtain the direction of arrival of a received signal, first task was design of a single reference rectangular patch antenna which resonates at 10 GHz frequency. A rectangular shape is selected as it has better impedance bandwidth in contrast to others. The same parameters are used as the HRR coupler i.e. the substrate type, its relative permittivity and thickness of the substrate. Utilizing the transmission line model of patch antenna design, initial dimensions of the patch antenna were obtained. The model of the reference rectangular patch antenna with the quarter wave transformer (QWT) feed method was designed. Its model was drawn in CST and TRF optimization method was applied to adjust the dimensions

so that the antenna resonates at 10 GHz operating frequency. Based on the optimized dimensions in Table 3.2, the layout of the model is shown in Figure 3.2.

Table 3.2: Optimized dimensions of rectangular patch antenna

Parameter	dimension
Operating frequency (f)	10 GHz
Permittivity of the substrate (ε_r)	3.23
Substrate height (hs)	0.85 mm
Length	7.712 mm
Width	10.1 mm
Width of microstrip feed (fw)	0.566 mm
Width of microstrip 50Ω feed (fw50)	2.073 mm
length of microstrip feed (lw)	4.6287 mm
length of microstrip 50Ω feed (lw50)	1.419 mm

The layout patch antenna with the dimensions indicated is shown in

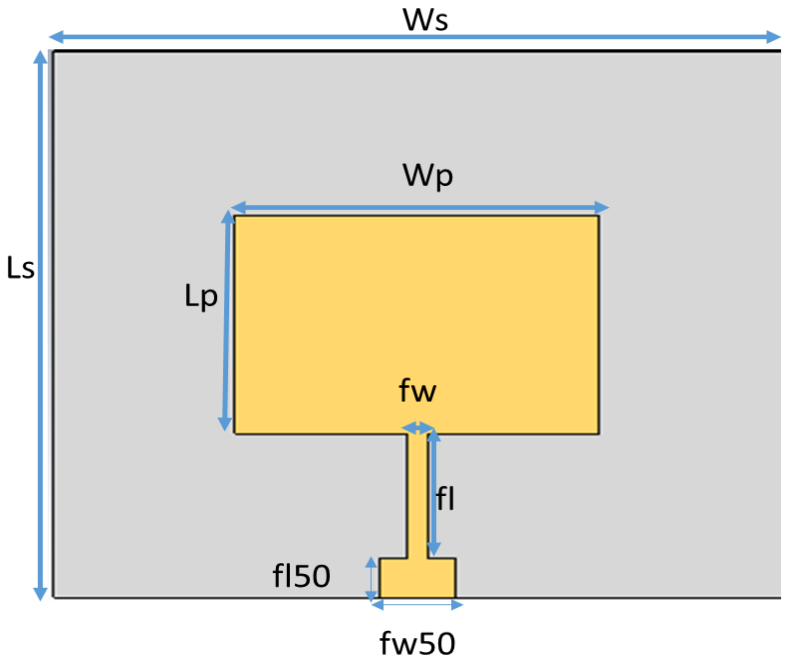

Figure 3.2: Patch antenna model

3.3 2x1 Rectangular Patch Antenna Array Model

A 2x1 rectangular patch antenna array is designed to estimate the angle of arrival received from the 180^0 HRR coupler. A 2x1 patch antenna array is selected to integrate with the 180^0 HRR coupler's two input ports. Two approaches were applied in modeling the antenna array in order to understand the effect mutual coupling between the individual antennas. The first method was designing of the antenna array that has the same dimensions as the reference rectangular patch antenna with inter-element separation distance of 0.6λ (λ is the operating frequency wave length) as shown in Figure 3.3. The second approach was reducing the inter-element separation to 0.4λ as depicted in Figure 3.4 which makes the antenna system more compact.

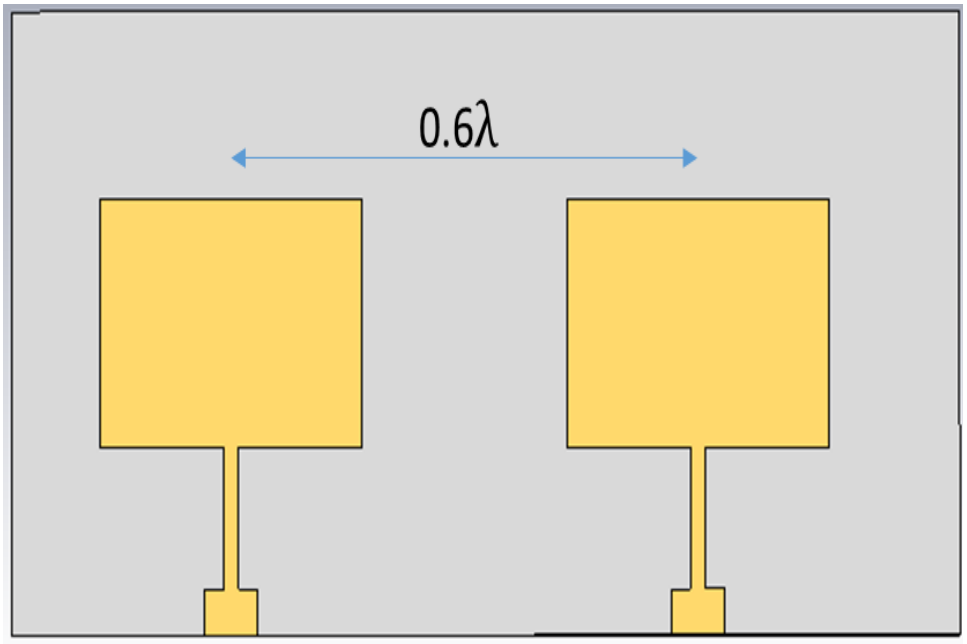

Figure 3.3: 2x1 rectangular patch antenna array with inter-element separation 0.6λ

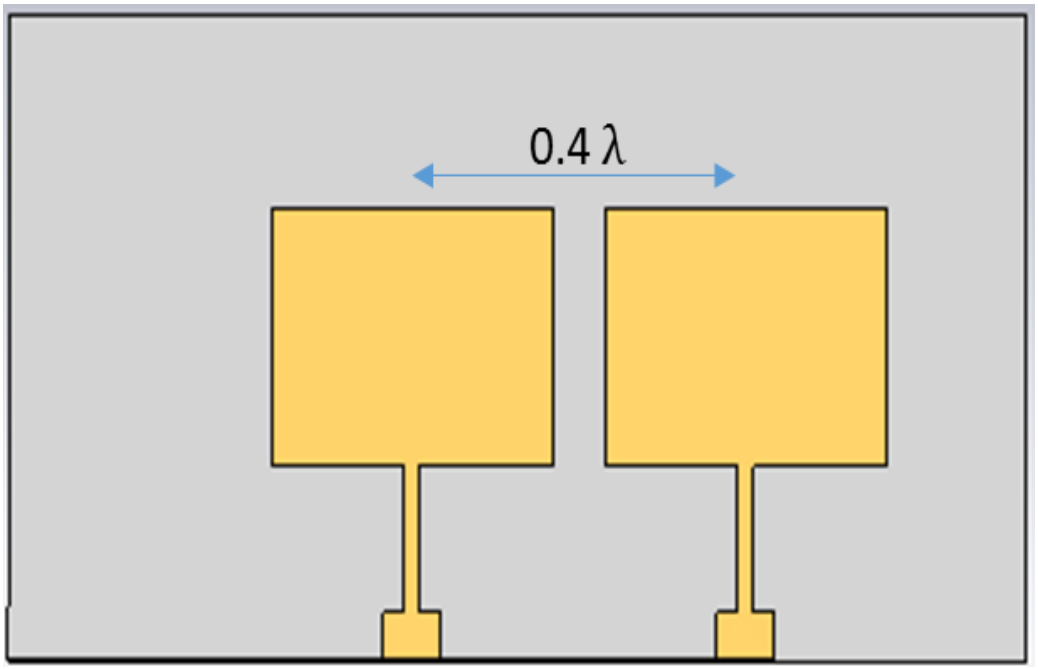

Figure 3.4: 2x1 rectangular patch antenna array with inter-element separation 0.4λ

3.4 2x1 Rectangular Patch antenna array integrated with HRR coupler Model

In this configuration, the HRR coupler was integrated with rectangular patch 2x1 array antenna to estimate the angle of arrival of a received signal. All the dimensions of the antenna array and coupler are optimized for better performance using CST studio software. As shown in Figure 3.4, At sum port (Σ) the signal from the two antennas is added in phase. On contrast, at the difference port(Δ) the signals received from the antennas added and results in a phase difference 180^0.

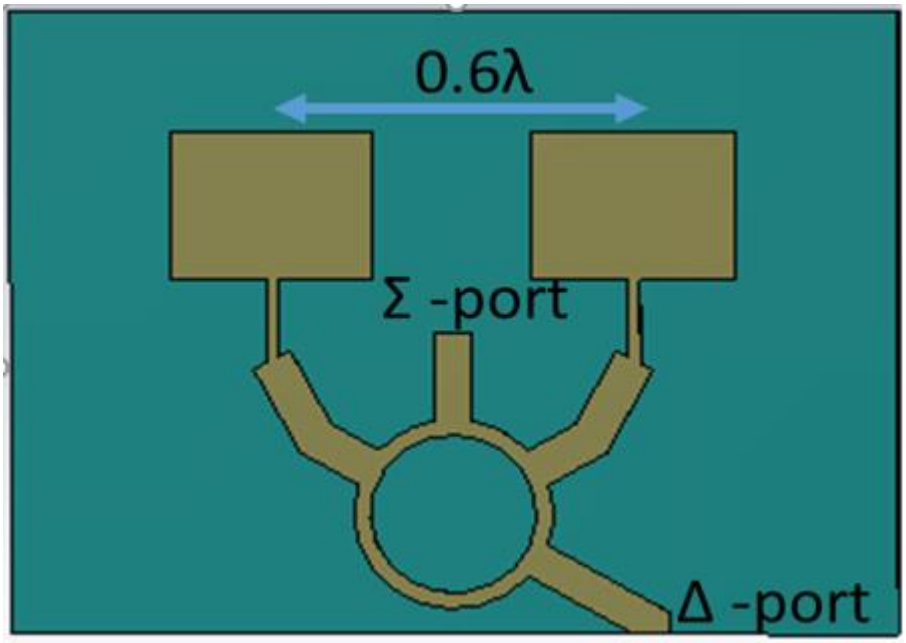

(a) Inter-element separation 0.6λ

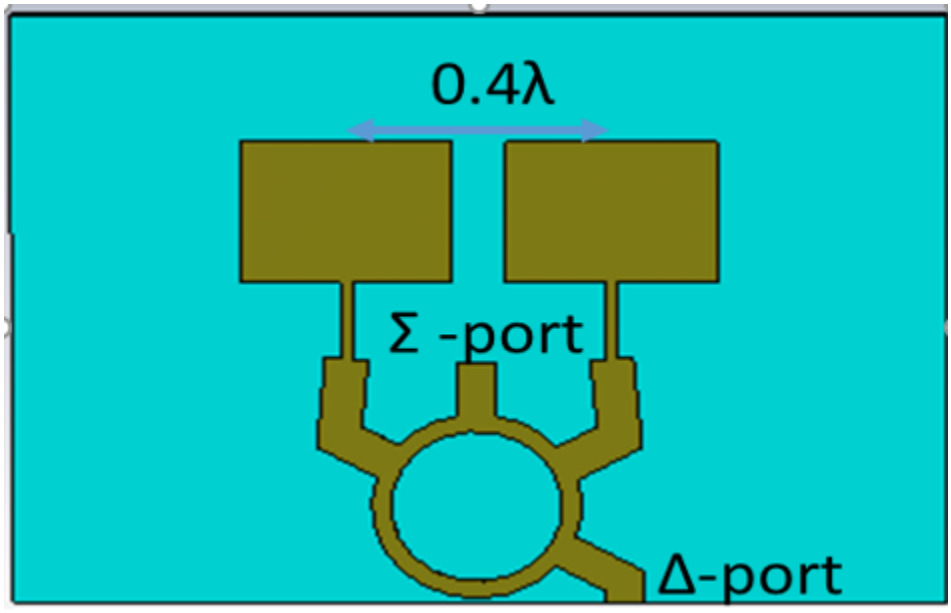

(b) Inter-element separation 0.4λ

Figure 3.5: 2x1 antenna Array antenna with HRR coupler with inter-element separation (a) 0.6λ and (b) 0.4λ

3.5 Square SRR Model

The optimized dimensions of a square split ring resonator (SSRR) unit cell metamaterial that exhibits negative permeability property are described in Table 3.3. Using the dimensions, the lay out model for the SSRR was designed in CST as it is shown in Figure 3.5.

Table 3.3: SSRR optimized dimensions

Parameter	dimension
Operating frequency (f)	10 GHz
Permittivity of the substrate (ε_r)	3.23
Substrate height (hs)	0.85 mm
Length or width (Ls = Ws)	2.407 mm
Outer ring length (Lo)	0.566 mm
Inner ring length (Li)	2.073 mm
Space (S)	0.1507 mm
Width (w)	0.2079 mm
Gap (g)	0.185 mm
Length of superstrate substrate (Lsup)	22.85 mm
Width of superstrate substrate (Wsup)	27 mm
Inter-element gap (g)	0.46 mm
Distance between the substrates (h)	4.328 mm

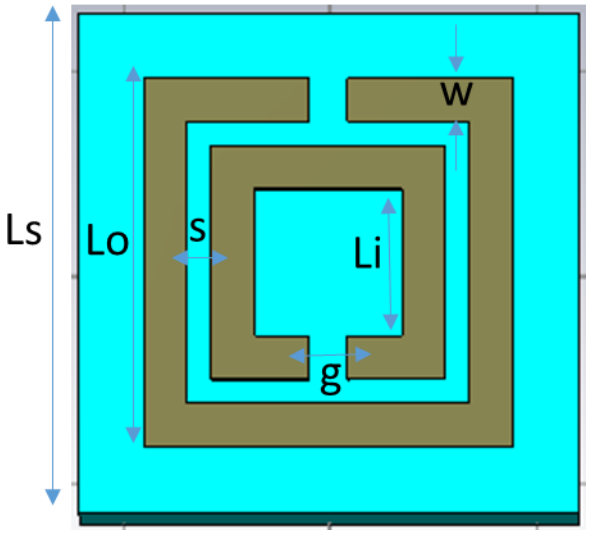

Figure 3.6: SRR model

A special boundary conditions were applied to the SSRR unit cell metamaterial to extract the constitutive parameters. The arrows in Figure 3.7 indicate, magnetic and electric boundary conditions in the z and y-planes respectively while the wave port excitation is represented through the x-plane.

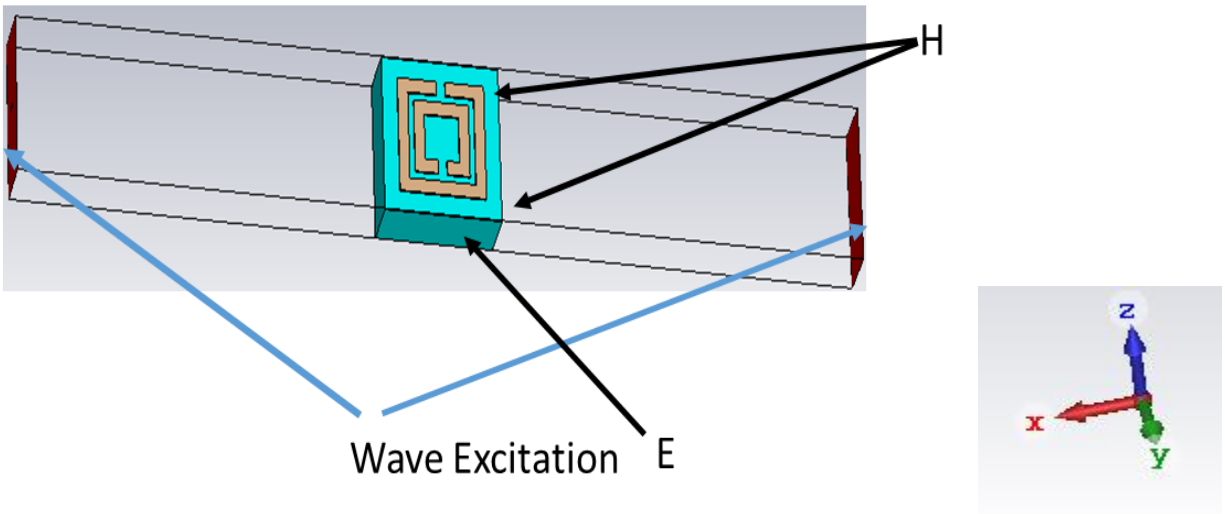

Figure 3.7: SSRR model in a waveguide placed under special boundary conditions

The unit cell SSRR model is arranged in a 9x5 array fashion as it can be observed in Figure 3.7, to be placed as superstrate in the final model of the work. The 9x5 array configuartion is selected to fit the rectangular shape of the patch antenna. Moreover, the configuration demonstrates optimal performance; where as other type of arrangment causes to reduce the performance the design.

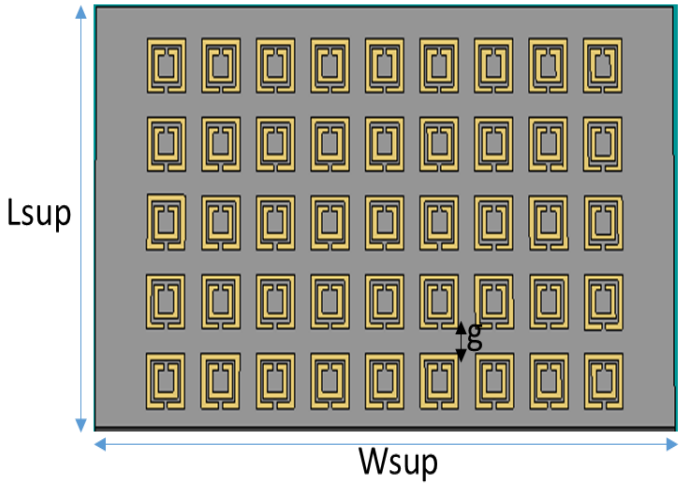

Figure 3.8: 5x9 SSRR model

3.6 180^0 HRR Coupler, 2x1 Rectangular Patch Antenna Array with Square SRR Superstrate Model

The final model of the antenna includes the HRR coupler, 2x1 rectangular patch antenna array and the 5x9 SSRR array placed at a height, h=3.15 mm from the substrate as can be seen from Figure 3.8. In this model the inter-element space between the patch antennas is 0.4λ. This distance suggests how much the antenna system is miniaturized without compromising the performance.

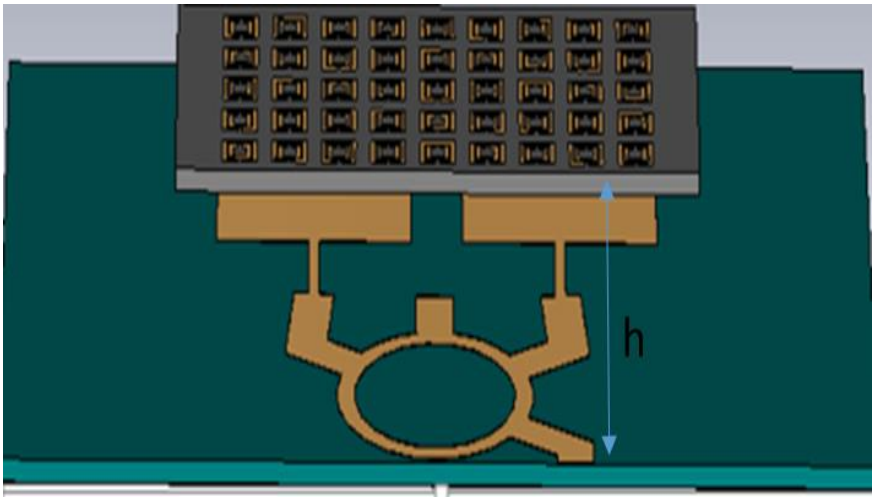

Figure 3.9: 2x1 rectangular patch antenna array integrated with HRR coupler and superstrate 5x9 SSRR metamaterial

Chapter 4

Simulation Results and Discussions

In this chapter, simulation results obtained from the CST software are provided. Based on the obtained simulation results, a through discussions are included. The operating frequency, height of substrate, permittivity are common simulation parameters for all the designs. These common simulation and other specific parameters are stated in Table 4.1.

Table 4.1: Simulation parameters

Parameter	value
Operating frequency (f)	10 GHz
Permittivity of the substrate (ε_r)	3.23
Substrate height (hs)	0.85 mm
Inner radius for coupler (r_{in})	4.11 mm
Outer radius for coupler (r_{out})	4.94 mm
Inter element distance between patch antennas(d)	0.4λ, 0.6λ
Outer ring length of SSRR (Lo)	0.566 mm
Inner ring length of SSRR (Li)	2.073 mm
Space between SSRR unit cells (S)	0.1507 mm
Width of SSRR (w)	0.2079 mm
Gap of SSRR (g)	0.185 mm
Length of patch	7.712 mm
Width of patch	10.1 mm

4.1 180^0 HRR coupler Simulation Results

As discussed in Chapter 3, the 180^0 HRR coupler model was designed to work in 10 GHz frequency. This frequency is selected so that it works for estimating angle of arrival in satellite communication. The 180^0 HRR coupler was analyzed using an electromagnetic field simulator, i.e. CST. The return loss coefficient curves of each port (S11, S22, S33, S44) for the coupler is given in Figure 4.1. A good matching condition for each port was satisfied with reflection coefficient of almost -40.146 dB. The isolation coefficients between input ports as well as output ports (S12 and S34) are shown in Figure 4.2. They are approximately equal to -49.457 dB and -46.23 dB each port respectively.

The phase difference at the sum (Σ) and delta port obtained is shown in Figure 4.3(a) at 10 GHz frequency. There is small difference between the theoretical value and simulation results. This is caused by addition of small length to the two branches to suite the model so that wave excitation is applied to the ports properly. This small length in on of either the sum port or delta port causes a phase difference by itself. Hence, instead of obtaining 0^0 sum phase difference in the sum port approximately 8^0 phase difference was obtained. For similar reason, the phase difference at the delta port was deviated by approximately 7^0. Albeit, the small marginal difference, the angle of arrival estimation was not affected as it can be confirmed by the obtained simulation results as discussed in the next sections.

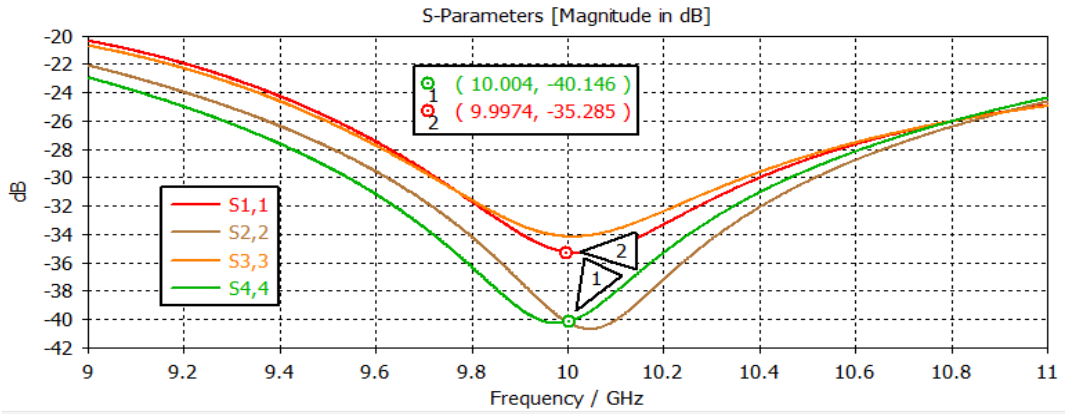

Figure 4.1: return loss

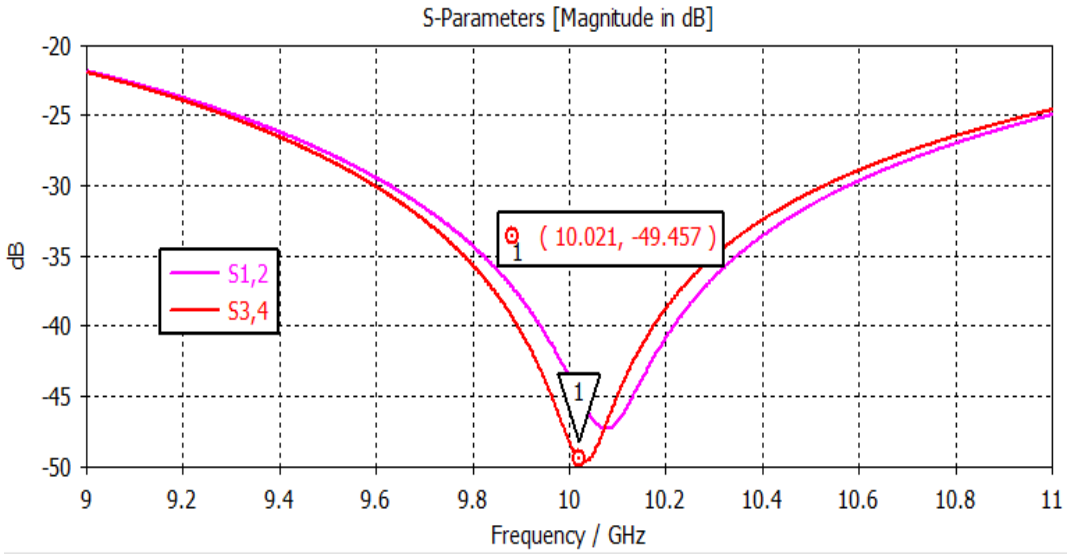

Figure 4.2: port isolation

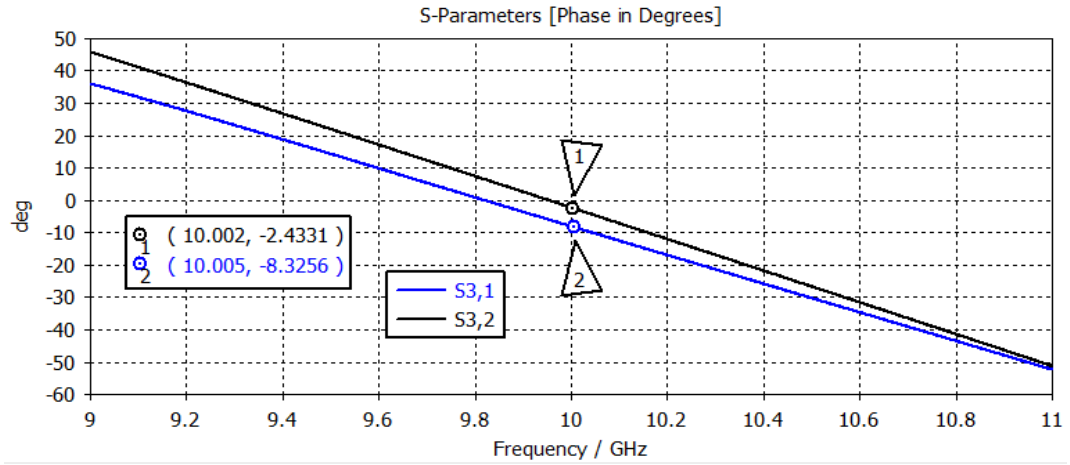

Figure 4.3: Phase difference at sum port

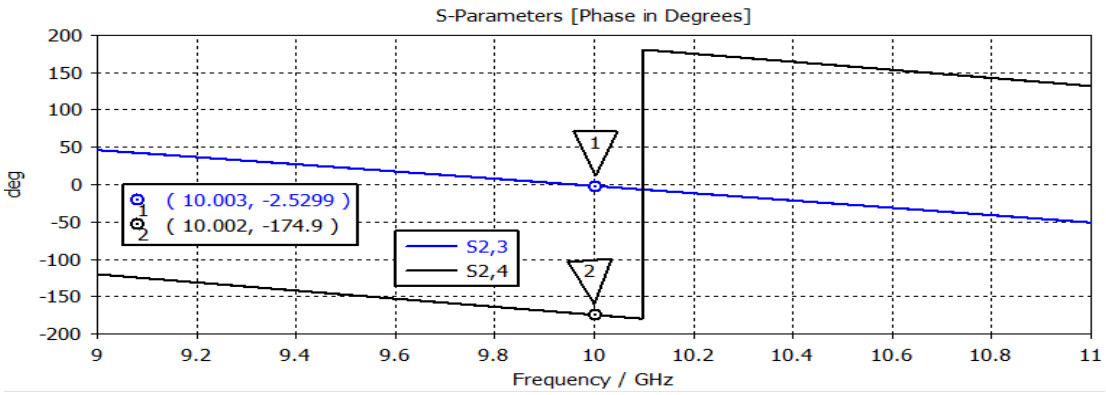

Figure 4.4: Phase difference at delta port

4.2 SSRR Simulation Results

The simulation results for the square split ring resonator (SSRR) unit cell metamaterial model is observed in Figure 4.5 and 4.6. Figure 4.5 shows the S- parameters of the SSRR unit cell metamaterial operates at 10GHz. Moreover, the real part permeability of the unit cell at the mention frequency is negative. This implies the unit cell metamaterial can be configured in an array fashion and applied as a superstrate to the 2x1 rectangular patch antenna- HRR coupler to improve the performance of the system.

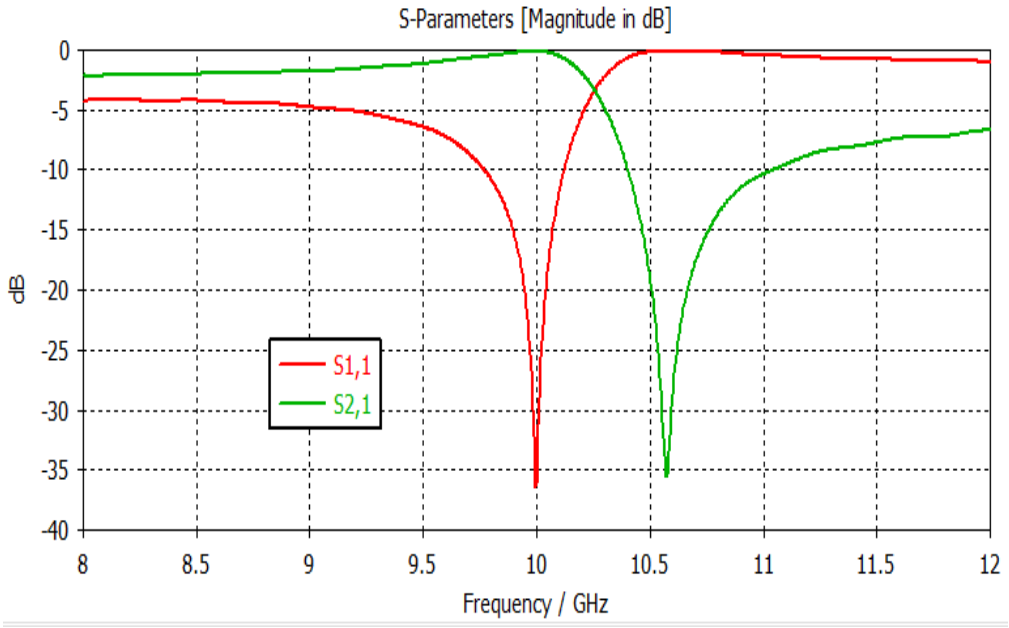

Figure 4.5: S-parameters of SSRR unit cell metamaterial

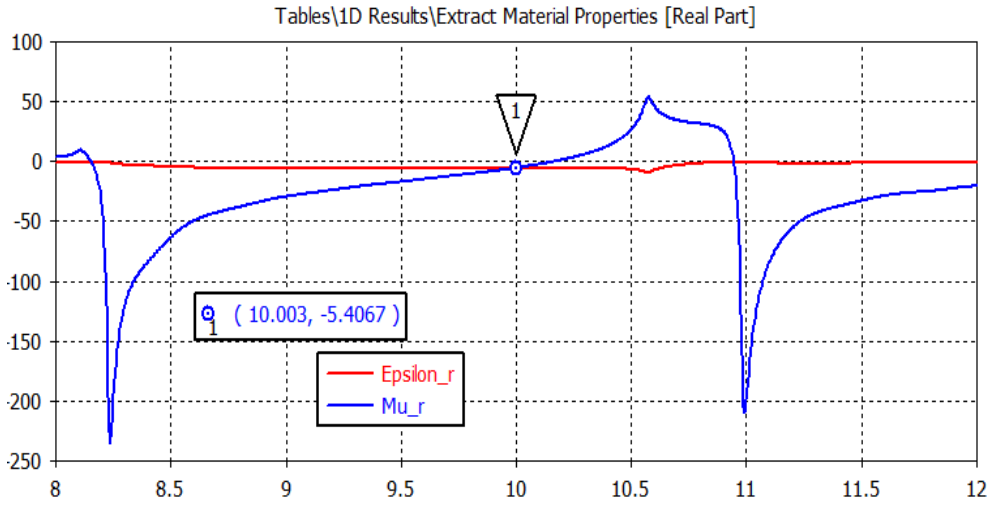

Figure 4.6: extracted epsilon and mu of SSRR unit cell metamaterial

4.3 Single Patch Antenna Results

After simulation was done on the single rectangular patch antenna, the antenna works as expected at 10 GHz frequency with a simulation return loss of -18.4 dB as indicated in Figure 4.1. It shows a bandwidth (BW) of 282MHz while the voltage standing wave ratio (VSWR) is 1.272 at the given operating frequency. Moreover, from Figure 4.3 radiation efficiency of 96.75% is obtained. This indicates a perfect match condition met between the antenna impedance and QWT feeder characteristics impedance. It also shows maximum gain of 6.403 dB both in the azimuth (phi = 0) and elevation planes (phi = 90) as observed from Figure 4.2 and 4.3. Moreover, the maximum power is transmitted towards the broadside direction.

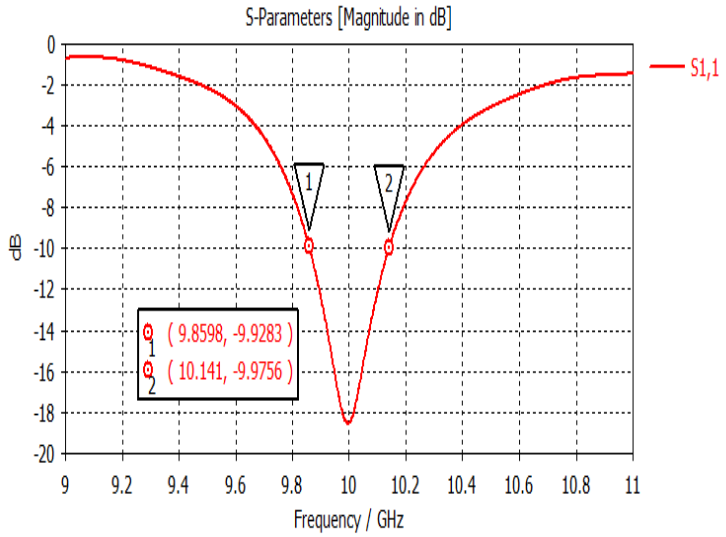

Figure 4.7: Return Loss

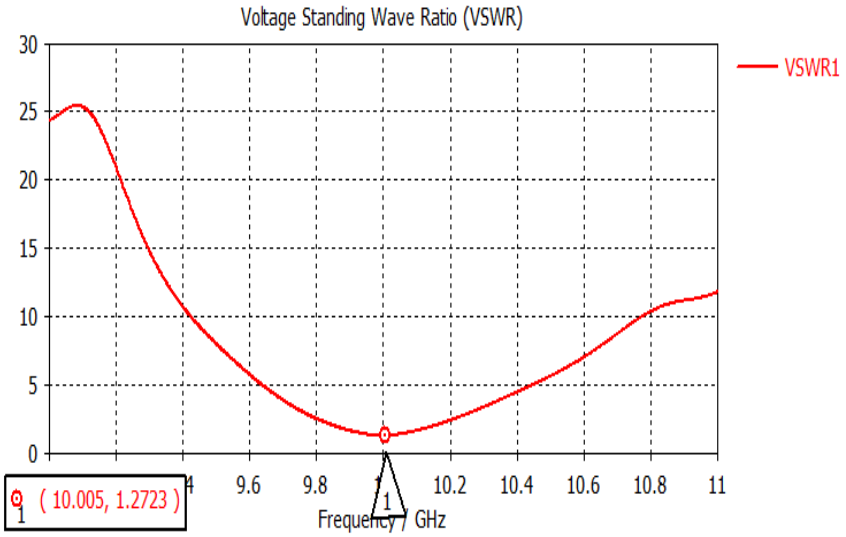

Figure 4.8: VSWR

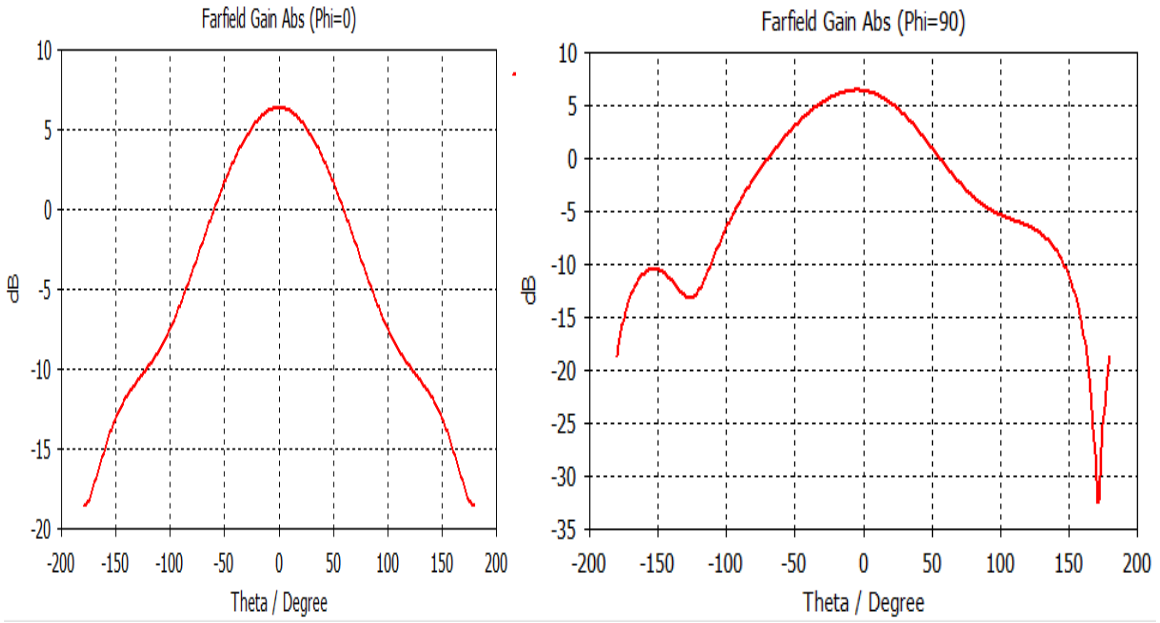

(a) (b)

Figure 4.9: Gain (2D) (a) phi = 0 and phi = 90

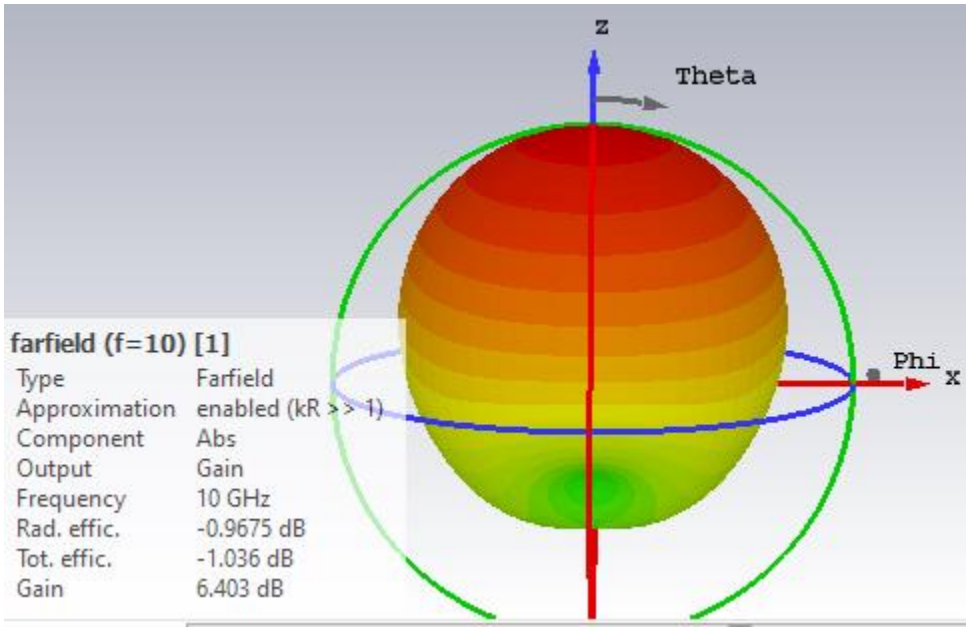

Figure 4.10: Radiation pattern (3D)

4.4 2x1 Patch Antenna Array Results (d = 0.6 λ)

The reason why a 2x1 patch antenna selected is to fit the two input ports when combined with the 180^0 HRR coupler. Though it is possible to design 2x2 or more array patch antenna system, it contrasts our main objective of designing a compact in size antenna system.

The simulation results for 2x1 rectangular patch antenna are shown in Figure (4.4) -(4.5). Both antennas resonate at 10 GHz frequency showing a reflection loss of -25 dB. The mutual coupling between the antennas is obtained as -23 dB at the operating frequency. A significant change in the gain is observed compared to the single rectangular patch antenna. As noticed in Figure 4.5, a maximum gain of 8.824 dB in both the horizontal and vertical planes is observed. Whereas, the angle of maximum radiation pattern is unaffected in both cases. This implies that the mutual coupling between the antennas does not affect the performance.

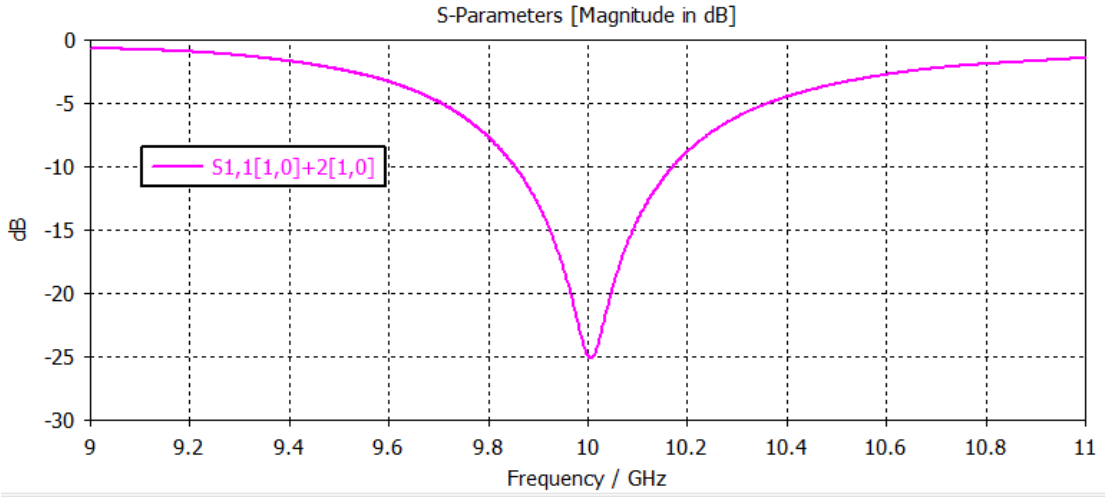

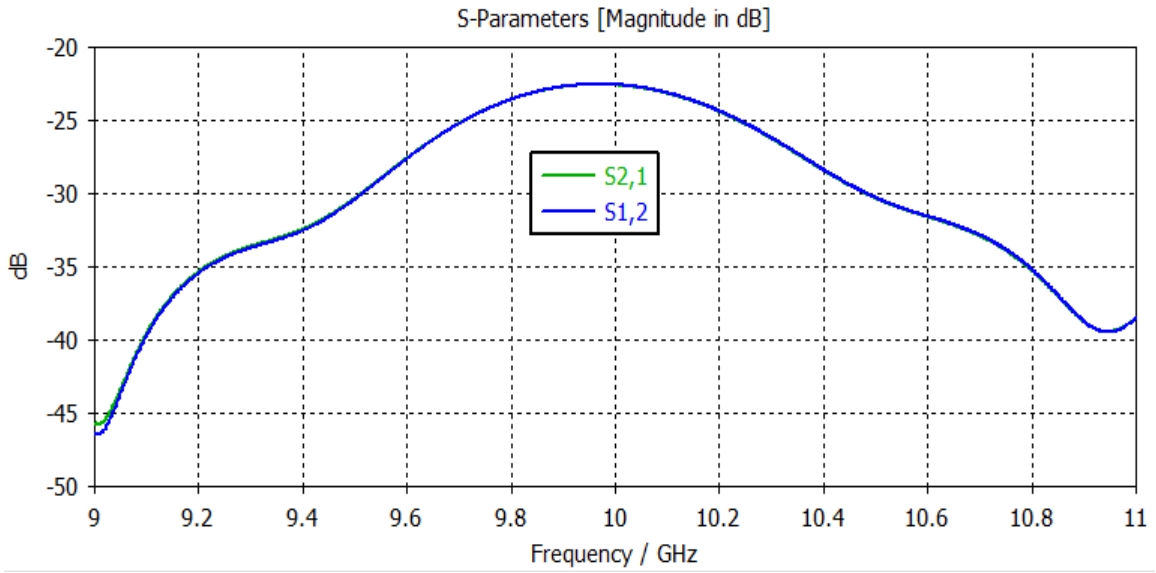

(a) (b)

Figure 4.11: Simulation results for 2x1 patch antenna array (d = 0.6 λ) (a) return loss (b) mutual coupling

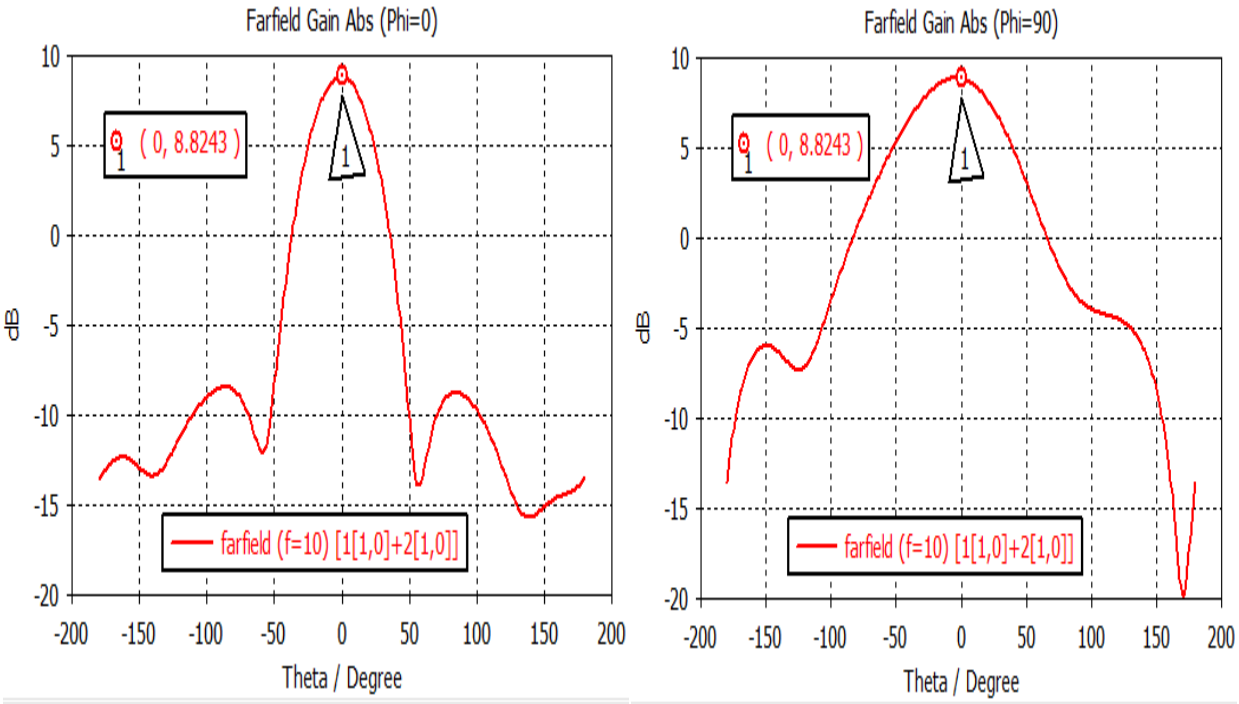

(a) (b)

Figure 4.12: Gain of 2x1 patch antenna array (a) phi = 0 (b) phi = 90

4.5 2x1 Rectangular Patch Antenna Array Results (d = 0.4 λ)

As it can be observed from Figure (4.6) -(4.7), the effect of mutual coupling becomes apparent when the inter element distance is 0.4 λ (where λ is operating frequency wave length). From the simulation results, the resonance frequency slightly shifted to the left while the return loss is maintained its original value. The mutual coupling between the antennas increased to -9 dB at the working frequency. The change in mutual coupling resulted in decreasing the gain from 8.824 (d = 0.64 λ) to 7.8 (d = 0.4λ) as shown in Figure 4.7 while maintaining its maximum radiation angles in both the azimuth (phi = 0) and elevation planes (phi = 90).

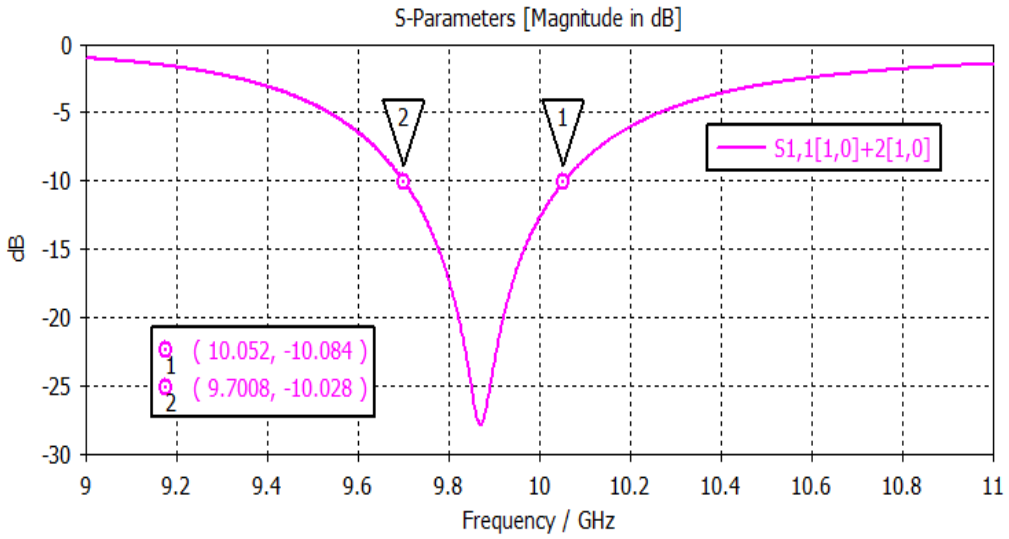

(a) return loss

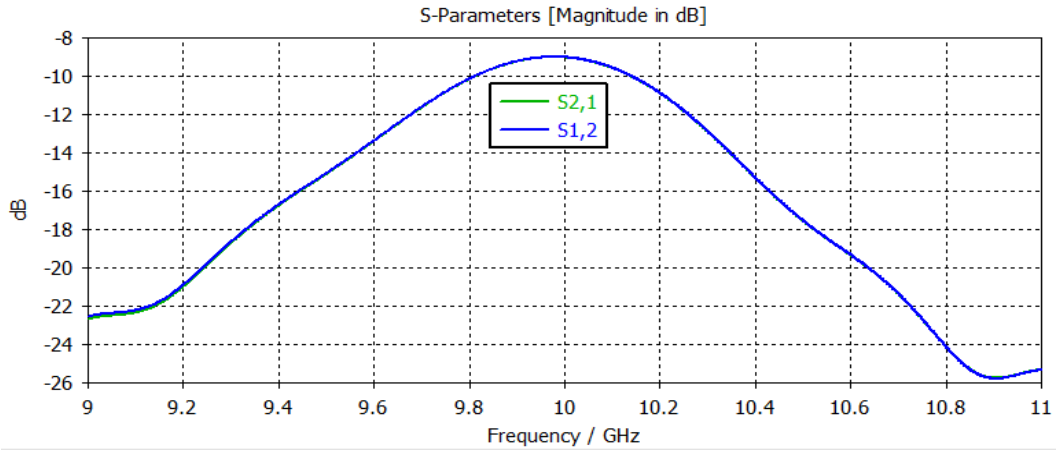

(b) mutual coupling

Figure 4.13: Simulation results for 2x1 patch antenna array (d = 0.4λ) (a) return loss (b) mutual coupling

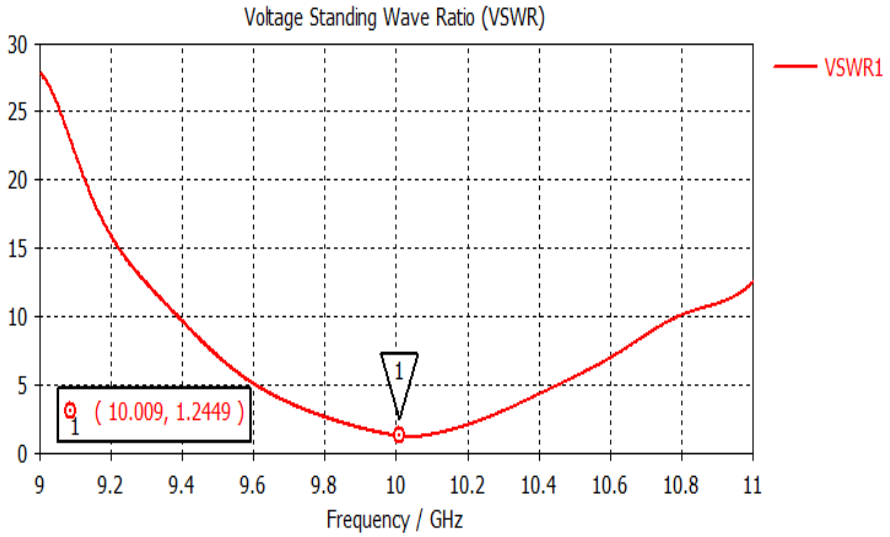

Figure 4. 14: VSWR

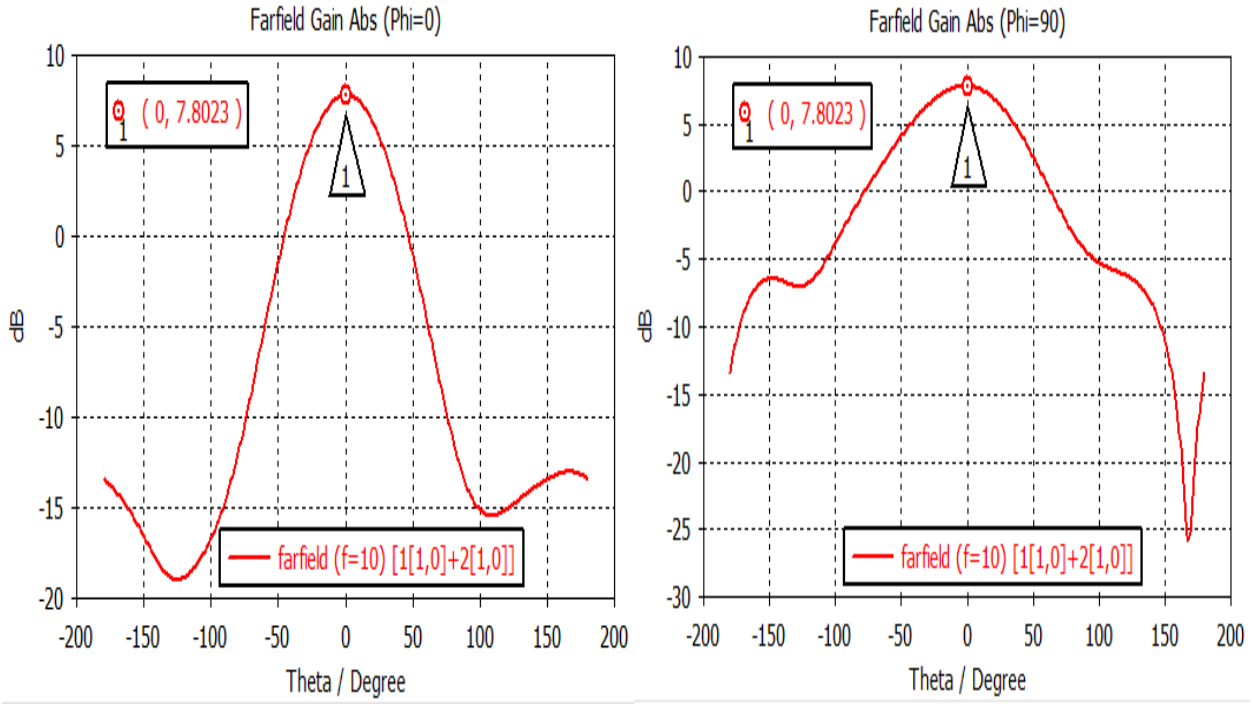

(a) (b)

Figure 4.15: Gain of 2x1 patch antenna array (d = 0.4 λ) (a) phi = 0 (b) phi = 90

4.6 2x1 Patch antenna array integrated with HRR coupler (d = 0.6 λ)

Figure 4.8 indicates, after integrating the coupler with the 2x1 patch antenna array, the return loss and mutual coupling are not affected as long as the inter-element spacing between the patches is 0.6λ. The antenna still resonates almost in the original frequency i.e. 10 GHz and the mutual coupling is maintained in the -23 dB bench mark.

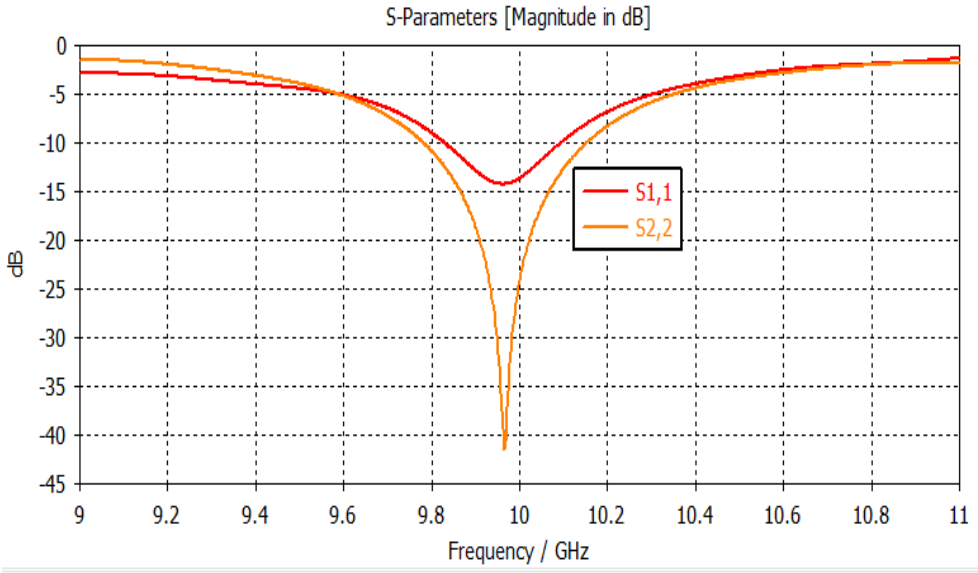

(a) S11

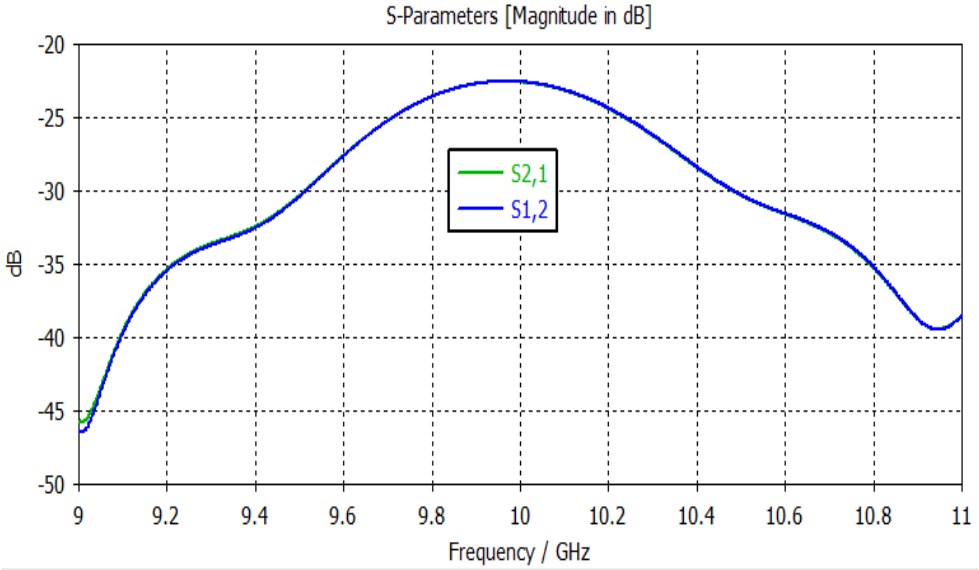

(b) S21

Figure 4.16: 2x1 Patch antenna array integrated with HRR coupler (d = 0.6 λ) (a) return loss (b) mutual coupling

Since there is adding in phase and out of phase by 180^0, there is some difference in the radiation pattern of the system as it is shown in Figure 4.9. However, the antenna system still has high gain without much affected by the integration of two systems.

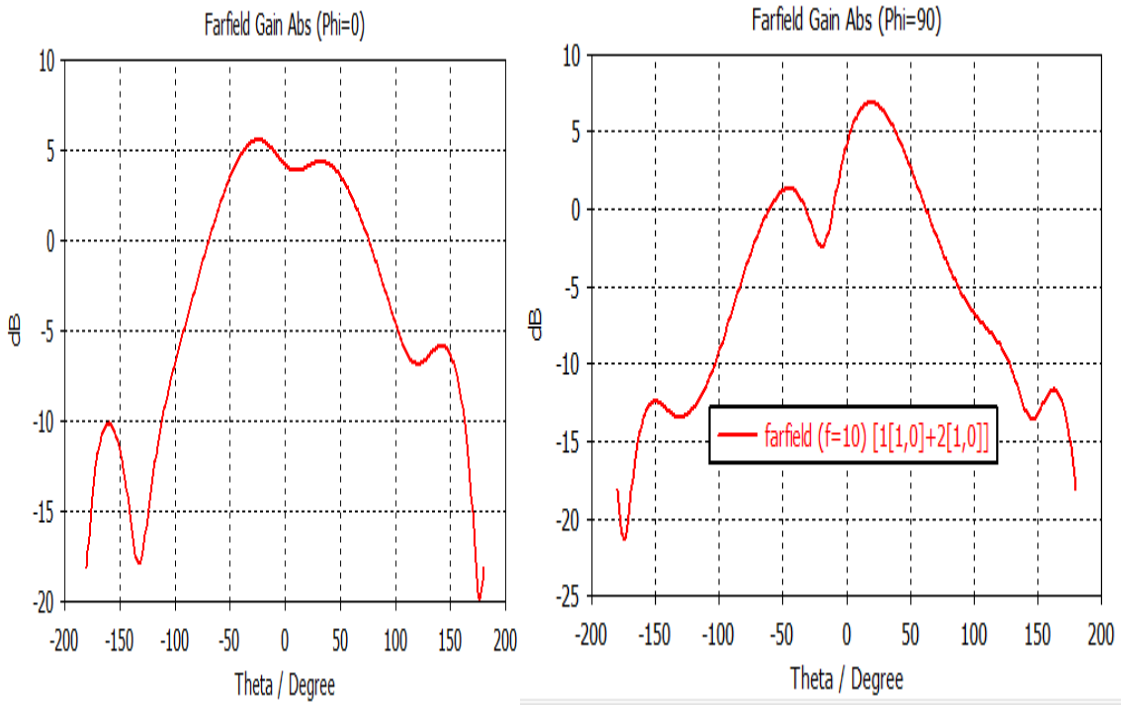

(a) Phi = 0 (b) Phi = 90

Figure 4.17: Gain of 2x1 Patch antenna array integrated with HRR coupler (d = 0.6 λ) (a) Phi = 0 (b) Phi = 90

The simulated normalized power obtained from the sum (Σ) and delta (Δ) ports is shown in Figure 4.10. It indicates a maximum value in the sum port while showing minimum value at the delta port.

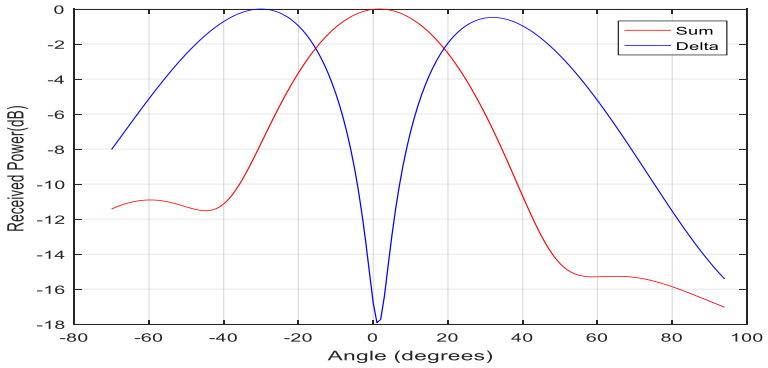

Figure 4.18: Normalized power of a 2x1 Patch antenna array integrated with HRR coupler (d = 0.6λ)

In Figure 4.11, the 2x1 patch antenna array -180^0 HRR coupler system was able to estimate the DoA of the received signal from 0^0 to 19^0 with error of less than 5^0 [29].

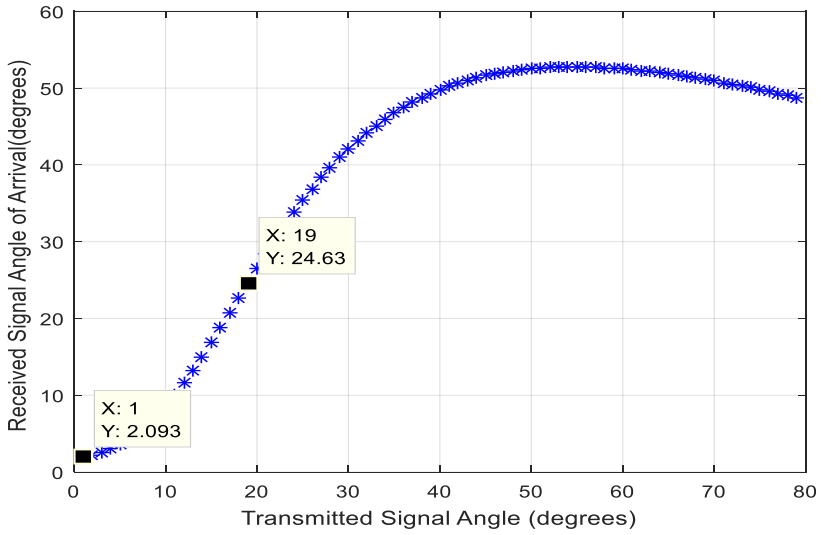

Figure 4.19: Angle of arrival of a 2x1 Patch antenna array integrated with HRR coupler (d = 0.6λ)

4.7 2x1 Patch antenna array integrated with HRR coupler Results (d = 0.4λ)

The simulation result in Figure 4.12 displays, the return loss and mutual coupling after combining the coupler with the 2x1 patch antenna array by decreasing the spacing distance, d to 0.4λ. As it can be shown from the figure, the results for return loss and mutual coupling are affected significantly. The antenna resonates in the frequency of 9.9GHz and the mutual coupling increased to -9dB. The obtained mutual coupling does not satisfy the -12dB mutual coupling coefficient and affects the performance of the system.

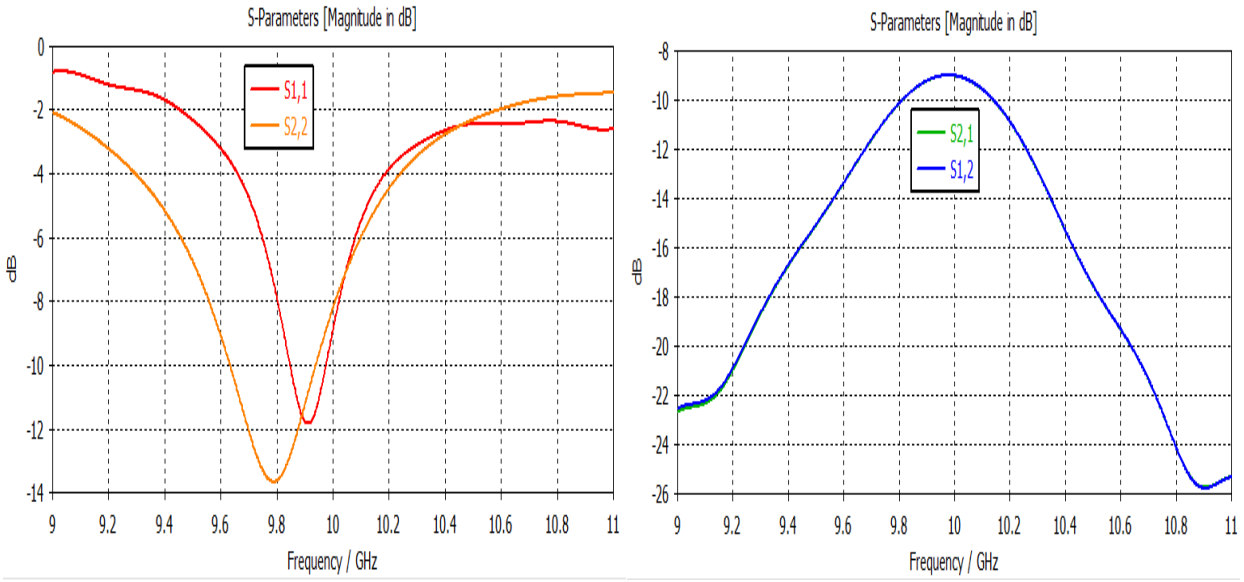

Figure 4.20: 2x1 Patch antenna array integrated with HRR coupler (d = 0.4λ) (a) return loss (b) mutual coupling

As a result of the high mutual coupling between the antennas, the radiation pattern as shown in Figure 4.13 is degraded.

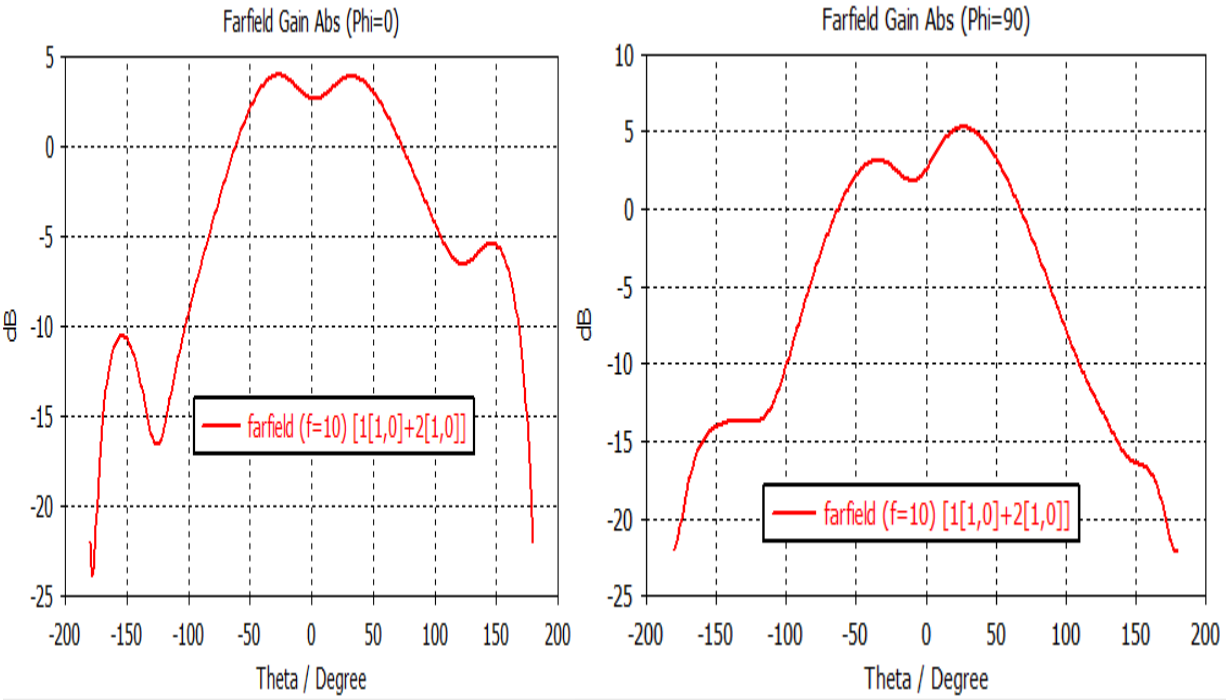

Figure 4.21: Gain of 2x1 Patch antenna array integrated with HRR coupler (d = 0.4λ) (a) Phi = 0 (b) Phi = 90

Whereas the simulated normalized power obtained from the sum (Σ) and delta (Δ) ports is shown in Figure 4.14 still keeps its minima and maxima points at the same angle.

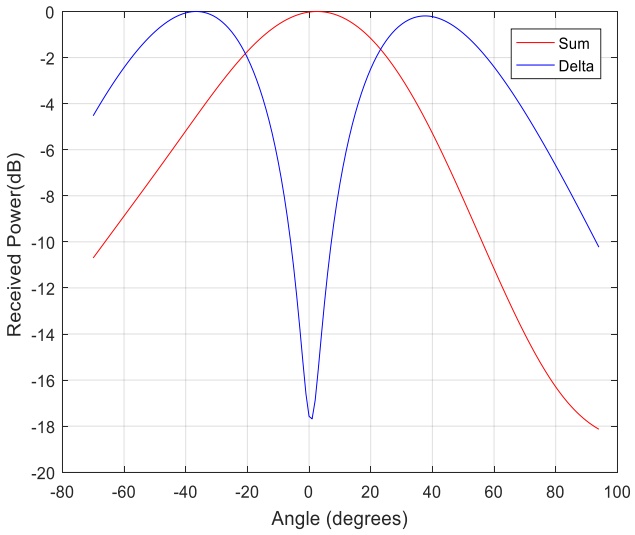

Figure 4.22: Normalized power of a 2x1 patch antenna array integrated with HRR coupler (d = 0.4λ)

The 2x1 patch antenna array -180^0 HRR coupler system was able to estimate the DoA of the received signal from 0^0 to 50^0 with error of less than 5^0 [29] as indicated in Figure 4.15 by decreasing the spacing distance, d to 0.4λ.

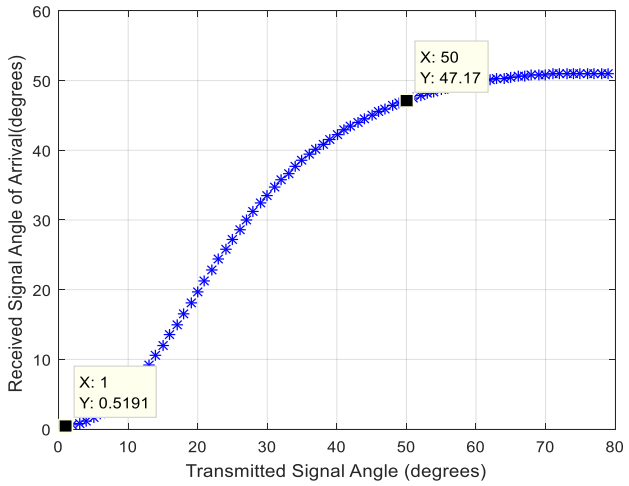

Figure 4.23: Angle of arrival of a 2x1 Patch antenna array integrated with HRR coupler (d = 0.4λ)

4.8 2x1 Patch antenna array integrated with HRR coupler and SSRR Superstrate (d = 0.4λ)

Figure 4.16 shows the simulation mutual coupling result after 5x9 SSRR metamaterial is placed as a superstrate to the closely spaced (d = 0.4λ) antenna array- HRR coupler system. The result implicates the mutual coupling is improved by 7 dB after the SSRR is placed over the antenna array-HRR coupler system by keeping the spacing distance between the patch antennas to 0.4λ.

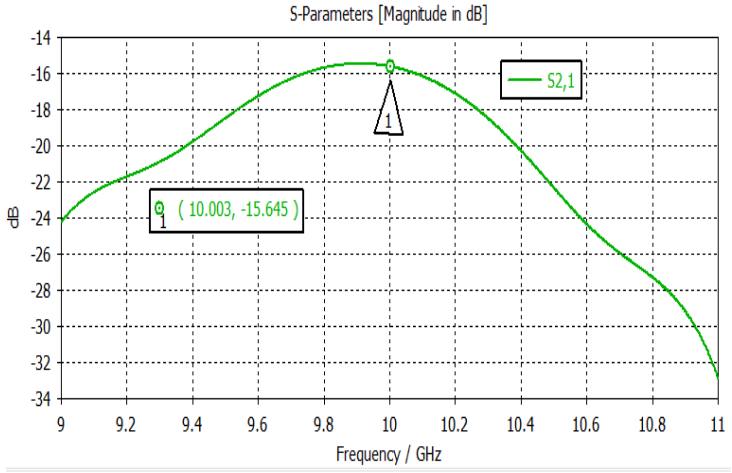

Figure 4.24: 2x1 patch antenna array integrated with HRR coupler and 5x9 SSRR metamaterial array superstrate (d = 0.4λ) mutual coupling

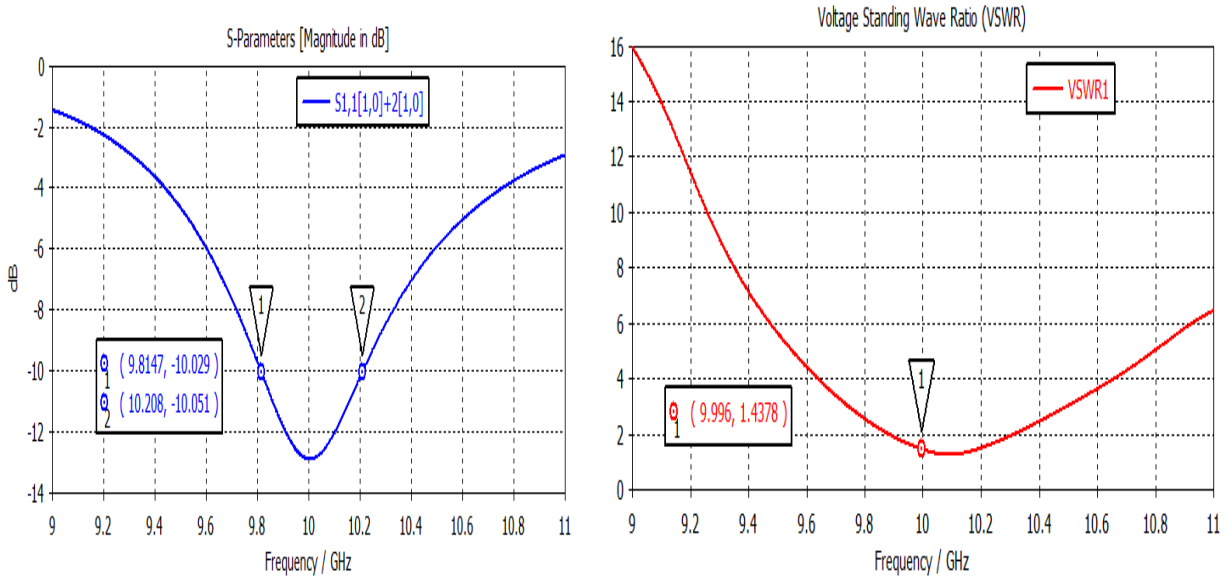

(b) (b)

Figure 4. 25: return loss(a) and VSWR (b)

The simulated normalized power obtained from the sum (Σ) and delta (Δ) ports is shown in Figure 4.17. The SSRR did not affect the maximum value in the sum port and the minimum value at the delta port.

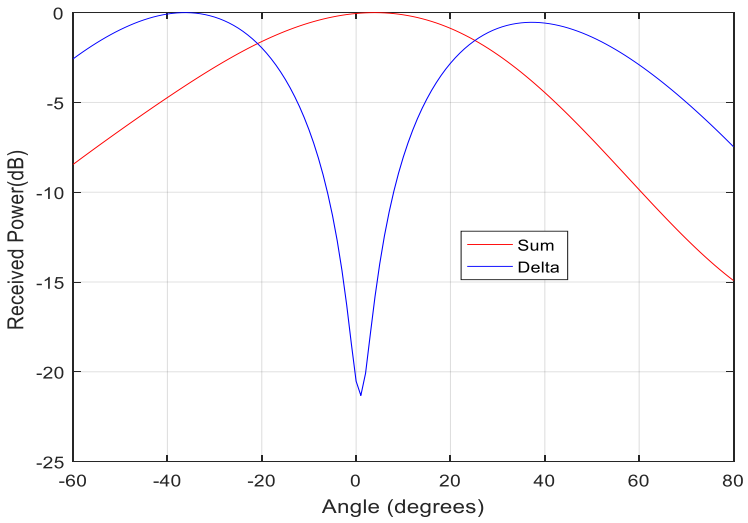

Figure 4.26: Normalized power of a 2x1 patch antenna array integrated with HRR coupler and 5x9 SSRR metamaterial array superstrate (d = 0.4λ).

After placing the 5x9 SSRR metamaterial array to the 2x1 patch antenna array -180^0 HRR coupler system, it was able to estimate the DoA of the received signal from 0^0 to 46^0 as shown from Figure 4.18(a). Moreover, Figure 4.18(b) indicates the rms error of the estimation in that angle of arrival range is close to 5^0 [29].

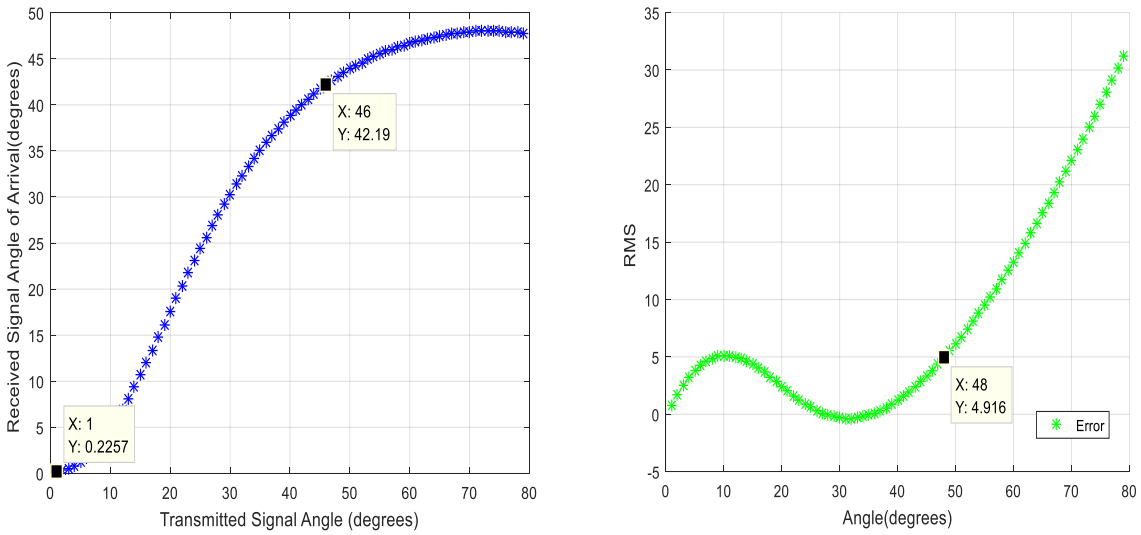

(a) (b)

Figure 4.27: 2x1 patch antenna array integrated with HRR coupler and 5x9 SSRR metamaterial array superstrate (d = 0.4λ) (a) angle of arrival (b) rms error

4.9 Result Summery

Table 4.1 summarizes the simulation results for all the discussions in this chapter. As it can be observed from the table, the 2x1 patch antenna array integrated with the HRR coupler and an SSRR metamaterial superstrate shows better results comparing to the designs. It shows better mutual coupling, gain and optimum range of estimating angles of arrival.

Table 4.2: Result summary

Design	Return loss (dB)	Mutual coupling (dB)	Gain (dB)	Estimated AoA (^{0})	RMS error (^{0})

Single rectangular patch antenna	-23	-	6.403	-	-
2x1 patch antenna array (d =0.6λ)	-25	-23	8.84	-	-
2x1 patch antenna array (d = 0.4λ)	-27	-9	7.8	-	-
2x1 patch antenna array + HRR coupler (d =0.6λ)	-15	-23	6.4	0-19	< 5
2x1 patch antenna array + HRR coupler (d = 0.4λ)	-12	-9	5.2	0-50	< 5
2x1 patch antenna array + HRR coupler + 5x9 SSRR (d = 0.4λ)	-14	-15.645	6.4	0-46	< 5

Chapter 5

Conclusions and Recommendations

5.1 Conclusions

In this work, originally a single rectangular patch antenna was designed for reference purpose. Simulation was done and its performance was discussed in terms of return loss, efficiency and gain parameters.

To see the effect of mutual coupling in antenna arrays, a 2x1 rectangular patch antenna array with a spacing distance of 0.6λ was designed. After simulation, the patch antenna array shows a return loss of -25 dB with a mutual coupling of -23 dB at 10GHz operating frequency. Moreover, a maximum gain of 8.824 dB was observed. However, by decreasing the inter-element spacing distance to 0.4λ, a return loss of -27 dB with a mutual coupling of -9 dB at 10GHz operating frequency was obtained. The maximum gain obtained was 7.824 dB, decreased due to the mutual coupling effect.

For estimation of angle of arrival of a received signal, an 180^0 HRR coupler was designed. Simulation results for reflection loss, port isolations, and delta and sum port phase differences of the coupler were obtained.

A 2x1 patch antenna array integrated with the 180^0 HRR coupler was designed and analyzed for direction of arrival (DoA) applications. By fixing the inter element distance between the patch array antennas to 0.6λ and integrating with coupler, an angle of arrival 0^0 to 19^0 with error of less than 5^0. However, when the inter element spacing between the patches is decreased to 0.4λ, it was able estimate the DoA of the received signal from 0^0 to 50^0 with error of less than 5^0.

To mitigate the effect of mutual coupling, SSRR metamaterial was designed and analyzed. The constitutive parameters were retrieved. After placing the superstrate to the patch antenna array-HRR coupler system, significant improvement in terms of the mutual coupling was observed, numerically it improved by 7 dB. Moreover, the range of estimation of the angle of arrival of the system was not affected by the SSRR metamaterial superstrate.

5.2 Recommendations

The thesis work focusses only applying the direction of arrival in patch antennas. However, in the future work, to obtain better results:

- Dipole or other type of antennas could be used
- Instead of applying the SSRR metamaterial as a superstrate, it could be placed on the substrate of the patch

References

[1] G. G. Y. Y. Z. Chen, Introduction to Direction of Arrival Estimation, Artech House Publisher, 2010.

[2] S. Diagne et al., "Performance analysis of a system of localization by angle of arrival UWB radio.," *Int. J.Netw. Syst. Sci.* , , vol. 13, p. 15–27, 2020.

[3] H. K. Y. T. M. M. a. L. S. Jeong, "Gain-Enhanced Metamaterial Absorber-Loaded Monopole Antenna for Reduced Radar Cross-Section and Back Radiation," *Materials,* vol. 13, no. 6, pp. 1247-1253, 2020.

[4] A. K. P. Saxena, "Performance analysis of adaptive beamforming algorithms for smart antennas," *IERI Procedia*, vol. 10 , p. 131–137, 2014.

[5] A. S. e. al., "A comparative study of adaptive beamforming techniques in smart antenna using LMS and its variant," *International Conference on Computational Intelligent and Networks,* p. pp. 58–62, 2015.

[6] A. P. e. al., "Analysis of adaptive algorithms for digital beam forming in smart antennas," *International Conference on Recent Trends in Information Technology* , p. 64–68, 2011.

[7] J. C. B. Jo, "Direction of arrival estimation using non-singular spherical ESPRIT," *J. Acoust. Soc.*, vol. 143, no. 3, p. EL181–EL187, 2018.

[8] K. I. S. Iwazaki, "Extended beam forming by sum and difference composite co-array for real valued signals," *IEICE Trans. Fundam.*, Vols. W102-A(7), p. 918–925 , 2019.

[9] M. T. A. Ahmed, "Genetic algorithm based improved DOA Estimation using fourth-order cumulants.," *Int. J. Electron.*, vol. 104, no. 5, p. 747–760, 2017.

[10] W. D. M. Han, "Unconstrained robust adaptive beam forming with improved capon estimator," *IEEE MTTS International Wireless Symposium (IWS),* 2019.

[11] A. C.J. Lowrance, " Direction of arrival estimation for robots using radio signal strength and mobility,," *in Proceedings of the 2016 13th Workshop on Positioning, Navigation and Communications (WPNC),* 2016.

[12] F. Q. e. al., "Virtual multi-antenna array for estimating the angle-of-arrival of a RF transmitter," *inProceedings of the 2016 IEEE 84th Vehicular Technology Conference (VTC-Fall), Montreal, QC, Canada,* p. 1–5, 2016.

[13] I. D. e. al., " Angle of Arrival Estimation Using Deca-wave DW1000 Integrated Circuits.," *IEEE, Piscataway Township, NJ,* p. 1–6, 2017.

[14] A. W. A. N. A. Bole, "Chapter 1—basic radar principles," in *Radar and ARPA Manual*, Oxford, Butterworth-Heinemann, 2014, p. 1–28.

[15] N. K. C. Sun, " Direction of arrival estimation with a novel single-port smart antenna,," *EURASIP J. Adv. Signal Process.* , 2004.

[16] T. H. M.Z. Song, "Sum and difference multiple beam modulation transmitted by multimode hornantenna for inverse mono-pulse direction-finding," *Prog. Electromagn. Res.,* vol. 82, p. 367–380 , 2008.

[17] J. X. e. al., "Sum and difference beamforming for angle-doppler estimation with STAP-based radars," *IEEETrans. Aerosp. Electron. Syst.* , vol. 52, p. 2825–2836 , 2016.

[18] F. Y. e. al., "Single patch antenna with mono-pulse patterns.," *IEEE Microw. Wirel. Compon. Lett.* , vol. 26, no. 10, p. 762–764 , 2016.

[19] I. T. S.A. Shaikh, "Two axis direction finding antenna system using sum and difference patterns in X-band.," *Microw. Opt. Technol. Lett.* , vol. 57, no. 9, p. 2085–2092 , 2015.

[20] t. h.-t. v.-p. h. j. v. van-sang doan, "Phase difference measurment based angle of arrival estimation using long base-line interferometer," *IET Radar, Sonar & Navigation,* vol. 17, no. 3, pp. 449-465, 2023.

[21] S. K. W. W. Rustamaji, "The angle of arrival estimationof frequency - hooping cooprative object based on software-defined radio," *Scientific reports*, vol. 14, no. 4, p. 12, 2024.

[22] S. W. Z. Z. Aftab Khan, "A study of Angle of Arrival Estimation of a RF Signal with FPGA Acceleration," *2024 International wireless Communications and mobile Computing(IWCMC)*, vol. 10, no. 4, pp. 1625-1630, 2024.

[23] X. C. L. W. Xingjin Li, "Arrival Angle Estimation Based on Transfer Lerning in Complex Enivornments," *International Conferences on Innovative Computing and Cloud Computing*, vol. 10, no. 3, pp. 1354-1359, 2023.

[24] C. A. Balanis, Antenna Theory, Hoboken, New Jersey: John Wiley & Sons, 2005.

[25] D. L. Sengupta, "Approximate expression for the resonant frequency of a rectangular patch antenna," *Electron. Lett.*, vol. 19, no. 20 , pp. 834-838, 2007.

[26] R. Bancroft, Microstrip and Printed Antenna Design, SciTech Publishing, Inc ., 2009.

[27] D. M. POZAR, "Microstrip Antennas," *IEEE Proc. IEEE*, vol. 80, no. 3, p. 381–401 , 1992.

[28] T. S. Bird, "Definition and Misuse of Return Loss," *IEEE Antennas Propag. Mag.*, vol. 51, no. 2, p. 166–167, 2009.

[29] E. N. a. I. T. Ryo Tanaka, "A Mono-Pulse DOA Estimation Antenna," *IEEE*, pp. 1833-1834, 2014.

[30] D. M. Pozar, Microwave Engineering, Wiely & sons,, 1998.

[31] T. J. a. H. Neill, Complete Mathematics, Hachette UK Company, 2010.

[32] T. K. B. Peng, " Three dimensional angle estimation in dynamic indoor terahertz channels usingforward-backward algorithm," *IEEE Trans. Veh. Technol.*, vol. 66, p. 1–15, 2016.

[33] S. S. K.K. Sabb, "Application of an optimal stochastic Newton-Raphson technique to triangulationbased localization systems," *IEEE/ION Position, Location and Navigation Symposium (PLANS)*, p. 282–286, 2016.

[34] Y. H. i. R.J. Weber, "Analysis for Capon and MUSIC DOA estimation algorithms," *IEEE Antennas and Propagation Society International Symposium Conference*, p. 1–4, 2009.

[35] P. Gething, " Radio Direction Finding and Super resolution, Electromagnetics and Radar," *P. Peregrinus Ltd., London, ,* 1991.

[36] D. B. S.M. Sherman, "Mono-pulse principles and techniques," *Prog. Electromagn. Res. C*, , vol. 74, 2017.

[37] A. L. a. T. I. C. Caloz, "The challenge of homogenization in metamaterials," *New J. Phys.*, vol. 7, 2005.